JOURNAL OF MATHEMATICAL PSYCHOLOGY 41, 319–344 (1997)
ARTICLE NO. MP971177

Stability and Intermittency in Large-Scale Coupled Oscillator Models for Perceptual Segmentation

Cees van Leeuwen, Mark Steyvers, and Maarten Nooter

University of Amsterdam

The coupled map lattice, a system of locally coupled nonlinear maps, is proposed as a model for perceptual segmentation. Patterns of synchronized activity are obtained in the model from high-dimensional, deterministic chaos. These patterns correspond to segmented topographical mappings of the visual field. The chaotic dynamic has a dual role of contributing to pattern creation in unsynchronized states and of noise revolting against stabilization in synchronized states. The dynamic allows rapid transitions between unsynchronized and synchronized states. Their stability characteristics are explored using analytical tools and numerical simulations. Stability or instability are shown to be determined by network coupling strength, in proportion to the rate of chaotic divergence. The introduction of adaptive connections, in combination with stimulus-controlled oscillation, enables stable or meta-stable patterns of synchronized activity to occur, depending on the perceptual structure in the visual field. For a perceptually ambiguous pattern, the system switches between alternative meta-stable segmentations. The switching-time distribution obtained from the model was found in agreement with those observed in the experimental literature.

INTRODUCTION

Perceptual segmentation is a function of the visual system which facilitates the identification and localization of objects and events. In principle, there are many different ways to segment a given pattern of sensory activity but only some of them will be perceptually relevant. For finding these segmentations, computational heuristics have been proposed which operate according to principles of, among others, maximum curvature (Hoffman & Richards, 1984), uniform connectedness (Palmer & Rock, 1994), or the Gestalt principles of proximity and good continuation. A familiar problem with this approach is that these principles are not uniformly applicable. It depends on the situation, for instance, which of them has priority over the others. An alternative approach would involve segmentation determined by intrinsic, self-organizing properties of the system. Characteristically in such an approach, the optimal segmentation will be the one which is maximally *stable* (Kanizsa & Luccio, 1990).

Dynamic systems theory provides a framework for specifying the notion of stability. Dynamic systems are characterized by a vector $\mathbf{x}$ of state variables in a *state space*. The state variables evolve in continuous or discrete time along a trajectory through the state space, specified by equations. For systems operating in continuous time, these are coupled differential equations or a function $F\colon \delta\mathbf{x}/\delta t = F(\mathbf{x}, \mathbf{M})$, where $\mathbf{x}$ is the vector of state variables and $\mathbf{M}$ is a matrix of parameter values. For given parameter values a vector field is defined, which specifies the evolution of the system from each point in state space.

In a discrete-time dynamic system, the differential equations are replaced by equations of the form $\mathbf{x}_{t+1} = F(\mathbf{x}_t, \mathbf{M})$. What the vector field is for a continous-time dynamic system, is the return map for a discrete-time system. The return map describes for all points in state space and for a given set of parameter values the evolution of the system from the current state to the next. All the systems described in the present article are discrete-time systems. For this reason we will abbreviate for simplicity and call the units of $\mathbf{x}$ at time t: x_1, x_2, ..., x_n and use $x_i^{(1)}$ for $x_{i,\,t+1}$. We shall write x for x_t and $x^{(k)}$ for x_{t+k}. Similarly for the other time-dependent variables used in this article, we shall write s for s_t and $s^{(k)}$ for s_{t+k} and d for d_t and $d^{(k)}$ for d_{t+k}.

The stability of a discrete-time dynamic system can be characterized in terms of the properties of the return map. In some conditions, the system behavior will converge to a limit set. A limit set is a collection of one or more system states which have zero divergence in the map. Stable limit sets, or *attractors*, ave those limit sets for which all nearby states converge. Dynamic systems theory distinguishes static or point attractors, periodic, quasiperiodic, and strange attractors. The open set of states that converge to an attractor is called the *basin* of attraction. Instable limit sets, i.e., those for which all nearby states diverge, are called repellors. For some limit sets (for instance, a saddle point) convergence on one subspace of the model goes together with divergence on another. These limit sets are of particular interest for the subtle interplay between stability and instability observed in chaotic behavior.

Correspondence concerning this article and reprint requests should be addressed to Cees van Leeuwen, University of Amsterdam, Faculty of Psychology, Department of Psychonomics, Roetersstraat 15, 1018 WB Amsterdam, The Netherlands. E-mail: ceesvl@uvapsy.psy.uva.nl. The useful suggestions of Ionel Simionescu, Steve Link, Jim Townsend, and two anonymous reviewers are gratefully acknowledged.

0022-2496/97 $25.00

The concern with stability has led to extensive use of attractor dynamics (Amit, 1989) for the purpose of constructing models of perceptual systems (e.g., Grossberg & Mingolla, 1985). Exclusive concern with stability, however, may lead to a distorted view on perception. The inability to disengage attention from a stably established pattern, reflects a pathology of perception. It is likely from experience that our perception is governed by a dynamics which destabilizes perceptual patterns, which are becoming established. Even for a simple line drawing, for instance, prolonged viewing will lead to the predominant interpretation giving way to alternative ones, and this sometimes leads to the discovery of new and unanticipated forms (Martindale, 1995). For these reasons, besides stability, also flexibility must be a required of perceptual models.

A related phenomenon is consisting in the switchings that are observed between alternative interpretations of ambiguous figures like the Necker cube, the Schröder stairs, and certain regularly aligned dot patterns. These functional aspects once more illustrate the importance of *in*stability in the human perceptual system (Attneave, 1971). These observations suggest that perceptual systems have an internal homeostasis, which embodies a subtle interplay between those forces which approach and those which diverge from stably established perceptual patterns (cf. Skarda & Freeman, 1987). Ambiguous figures therefore provide an important tool for the study of human perceptual organization.

Whereas most models of perception have restricted themselves to settling on stable organizations (as in classical connectionism, for instance, Hinton, 1981), others have attempted to capture the interplay between perceptual stability and instability. Most of these approaches are based on the observation that switches between alternative organizations occur without conscious control. The neurally based satiation hypothesis originally proposed by Köhler (1940) is still today the most widely accepted explanation for perceptual ambiguity. Satiation can be conceived of as a process of gradual self-inhibition of a perceptual pattern. In this approach, negative feedback from its own state of activation causes the pattern to lose its attractiveness, ultimately leading to a transition to an alternative pattern.

The assumption of satiation is insufficient to explain the timing of the switching behavior. On the basis of neural satiation alone, perceptual states would alternate in regular cycles (Kawamoto & Anderson, 1985). Yet, the reversal times observed in experiments show considerable dispersion (De Marco, Penengo, Trabucco, *et al.*, 1977). To accomodate for this phenomenon, fluctuations have been imposed on the rate of satiation (Ditzinger & Haken, 1990a, 1990b). Fluctuations imply that satiation is a noisy process, but not that the destabilization is caused by the noise.

The assumption of an internal noise source has gained wide acceptance in the study of perceptual processes due to signal detection theory (Green & Swets, 1966). In this approach, the noise distribution is considered a stable property of the system. Noise in this view is caused by stochastic processes in the sensory channels which impose a random distribution onto a pure signal. Noise, in other words, attenuates the signal. The conceptual distinction between pure signal and stochastic noise of attenuating the signal is useful for applying information theory (Shannon & Weaver, 1949), but it has no basis in the physics of the signal, nor in experience. The commitment to the information processing approach, implied in using this distinction, in our view involves unnecessary restrictions on the use of dynamic systems theory for modelling perception.

In principle, noise could have a more productive role. To begin with, noise itself can be made responsible for escaping from a perceptual state. Noise can induce divergence from a stationary state, or from the trajectory that leads to an attractor. When noise is applied in this manner, it still is extrinsic to the system's attractor topology and has no other function than to attenuate information. This principle is familiar from the Boltzmann machine, in which it is used for avoiding that the system ends up in a spurious attractor, for instance a local minimum. The principle of using noise for escape has been used to model switching behavior (Hock, Kelso, & Schöner, 1993; Taylor & Aldridge, 1974).

According to these models, noise distribution is not a fixed channel property. The signal to noise ratio is manipulated in order to model a certain behavior. Control manipulations are necessary, because signal and noise still play opposite roles. The dynamics of the signal creates order and noise destroys it. Hence increasing the signal-to-noise ratio automatically implies less flexibility and vice versa; stability and flexibility are opposites. For instance, raising the level of noise in a Boltzmann machine architecture will facilitate escape when the system is caught in the basin of an attractor, but at the same time it involves a degeneration of the entire attractor landscape.

In these models, stability or instability is caused by the direct intervention of an external, strategic control process. A control schedule is needed to manage the proportion of signal and noise, for optimizing the behavior of the system in order to obtain stable and instable modes, whenever they are required. This solution violates both experiential and experimental constraints. In phenomenal experience, the switches occur spontaneously. In experiments, it has been shown that strategic control can influence switching behavior only in a nonspecific manner. It is possible to induce bias, in such a manner that one interpretation occurs more frequently than another, but the instruction to hold one interpretation cannot prevent the perceiver from switching to the other (Peterson & Hochberg, 1983).

Such facts are hard to accommodate for models which require direct control, as is ultimately the consequence of using the pure signal/stochastic noise distinction. Since these approaches are forced to make unrealistic assumptions

with respect to strategic control, it may be considered useful to explore alternatives. In the recent history of psychophysics, such alternatives have not often been considered, because prevalence was given to linear models. In linear models, stochastic assumptions are the only way to generate unpredictability. Alternative approaches to psychophysics have been proposed, however. These have advocated the use of nonlinear models and have proposed to ban stochastic noise from the psychological model to the outside world (Gregson, 1988), or even to abandon it completely (Gilden, Schmuckler, & Clayton, 1993). Alternatively with nonlinear models, deterministic chaos inside the system could be considered as a noise source (Gu, Tung, Yuan, Feng, & Narducci, 1984; Hogg & Huberman, 1984; Kaneko, 1983, 1984, 1989, 1990; Schult, Creamer, Henyey & Wright, 1987; Tsuda, 1992, 1993; Waller & Kapral, 1984; Yamada & Fujisaka, 1983).

The present article will present a model of perceptual destabilization and switching, based entirely on the notion of deterministic chaos. By proposing a chaos-based model, we wish to challenge the status of the conceptual distinction between pure signal and channel noise. An experience-based approach of perceptual organization which choses to remain agnostic with respect to information processing (as was proposed in van Leeuwen, 1989; in press; van Leeuwen & Bakker, 1995) might be served by not relying on this distinction. Chaos can be used as a noise source in patterns of activity, without having to treat their internal representations as information in the stochastic sense of the word.

The important advantage of chaos as a noise source will be, that extensive control schedules are no longer needed to acquire flexibility in a dynamic system. In traditional models, as a result of giving opposite functions to signal and noise, external control operations will always be needed for flexibility and so these models fall short of realizing the potentials of self-organization. In chaos-driven models, stability and flexibility are two sides of the same coin. Stable and unstable states can be found, arbitrarily close in the control space of the system, with the result that the problem of extrinsic noise management could be minimized. Chaotic dynamics therefore introduce a new perspective on noise, which may facilitate the effort to model the interplay of stability and instability of perception.

The heart of this new perspective is a property of nonlinear dynamics which Kelso (1995) brought to bear on the issue of perceptual switching between alternative interpretations. This property is called *intermittency*. Intermittency is an unstable state of activation. However, a model in the intermittent state will show apparently stable behavior for a certain time interval. In Kelso's (1995, p. 99) words: "In the intermittent regime, there is attractiveness, but, strictly spoken, no attractors." The attractiveness results in metastable states. A system in the intermittent regime appears to be caught in one of these states, but will always manage to free itself after a certain period. Kelso (1995) used intermittency to model the time course of switching behavior for ambiguous visual patterns. The model has two alternative meta-stable states, corresponding to alternative experiences. The system will get caught in one of these states, frees itself only to get caught in the other one. In this manner, the system continues to swing back and forth between alternative perceptual states.

In Kelso's (1995) approach, the dynamics of the perceptual system is described at the macroscopic level. The model has only a few degrees of freedom and a perceptual experience is represented by the value of a single variable. This level of description is insufficient, however, if we require a model to explain how a perceptual state could give rise to the experience of a complex, segmented pattern. For doing this, a microscopic level of description will be needed. A microscopic model may be less parsimonous for a particular case study and should therefore have significance for a wider range of phenomena. The proposed model should be able to produce switching behavior for ambiguous patterns as well as stable segmentation for a number of perceptually nonambiguous patterns.

The microscopic approach may follow Kelso (1995) in using intermittency to account for the switching behavior. Intermittency at macroscopic level can be obtained as the result of self-organization in distributed activity patterns. These patterns are to be understood as sensory activity. Noise in these patterns will have both a constructive and destructive role with respect to the emerging order. The noisy processes which help create the pattern will revolt against it, once it becomes established. The present article will investigate whether the stable and near-stable behaviors of simple systems can emerge in the complex system, by using both analytic techniques and numerical simulations. The simulations will provide a first approximation to a variety of segmentation behaviors of perceptual systems. Perceptually ambiguous and nonambiguous patterns are presented to the model. It will show stable behavior in the presence of nonambiguous patterns and intermittency in the presence of ambiguous ones.

The numerical simulations are intended as an approach to model brain functioning. Segmentation processes are assumed to take place in the primary visual cortex and beyond; they will operate as self-organization within a topographical image of the visual field (Hoffman, 1989). For simplicity, in the present research the visual cortex is modelled as a locally connected neural network in which there is a topographical mapping of the visual image. The problem of how to maintain coherence in such a distributed representation has become known as the binding problem. Given that the presently proposed model is such a distributed representation system, the self-organizing capacities of the system must solve the binding problem. Von der Malsburg and Schneider (1986) suggested that the synchronization of

neuron firing solves the binding problem. Such a solution also is adopted in the presently proposed model.

Evidence for synchronization of oscillatory activity in the visual cortex has been reported from animal studies. Initiated by Freeman's research (1975) on stimulus-induced oscillations in the olfactory bulb, studies in cat visual cortex by Eckhorn, Reitboeck, Arndt, and Dicke (1990), Engel, König, Gray, and Singer (1990), Gray, Engel, König, and Singer (1990) and Gray and Singer (1989) showed that neurons exhibit synchronous oscillations over relatively large areas and even between cortical areas. These neurons are topographically related to the retina. The frequency and amplitude characteristics of these synchronous oscillations in the visual cortex depend on feature attributes such as orientation, velocity, length, and coherence. For example, neurons with separate receptive fields oscillate in synchrony in response to two moving bars only if these bars have the same orientation. These results are in accordance with the suggestion that binding in the visual field is achieved by synchronization of oscillatory activity patterns.

Typically, models of synchronizing oscillatory activity use phase locking of periodic signals as a principle to acquire synchrony (Eckhorn *et al*., 1990; Grossberg & Somers, 1991; Sompolinsky & Golomb, 1991; Sompolinsky, Golomb, & Kleinfeld, 1990; Sporns, Gally, Reeke, & Edelman, 1989; Sporns, Tononi, & Edelman, 1991). Brain signals, however, do not show pure, harmonic oscillations. Rather, the activity is distributed across broad bands of the power spectrum and this could be interpreted as the effect of a high-dimensional chaotic system. Plausibility with respect to the spatio-temporal characteristics of neural activation patterns could therefore be claimed for a high-dimensional chaos-based model. In our view, oscillation is an intrinsic property of individual neurons, but regular, *periodic* oscillation is not. Regular 40–70 Hz oscillations may emerge as a combined effect of irregular ones as a result of feedback.

In sum, synchronization of oscillatory activity could be a collective variable in a model that shows stable and instable behavior, depending on whether the perceptual pattern is unambiguous or ambiguous. In the latter case, there will be intermittency, as in Kelso (1995). But other than in Kelso's work, it will be shown how these patterns of behavior could occur as the result of a self-organization in microscopic patterns of chaotic activity. The result will be a model which organizes perceptual patterns in a manner that is consistent with experience and is more realistic as a model of brain function than traditional stationary-attractor models or even the more recent oscillatory models which rely on stable phase coupling.

The introduction of the model requires two parts. In the first part, the stability characteristics of the model will be discussed. For the first part we rely strongly on the seminal work of Kaneko (1989, 1990). In the second part of the description, we will introduce adaptive coupling and oscillation functions which are applied to simulate perceptual segmentation behavior in nonambiguous and ambiguous conditions.

A first test of the model requires it to yield synchronized activity in accordance with principles of Gestalt organization, such as proximity and good continuation. In Fig. 1a, the pattern of dots is usually seen as two intersecting, continuing lines, to which a law of good continuation applies. In order to separate these two lines, at least one extra dimension is needed in the map. The dimension of orientation of the receptive fields in the model will serve for this purpose. Figure 1b will then be a testcase for this architecture since the circle is perceived as a continuing whole across different orientations and not as separate collections of oriented lines.

A model that can reach a stable segmentation for these perceptually unambiguous patterns, will show intermittent behavior in cases of ambiguous stimulation. In Fig. 2a, the

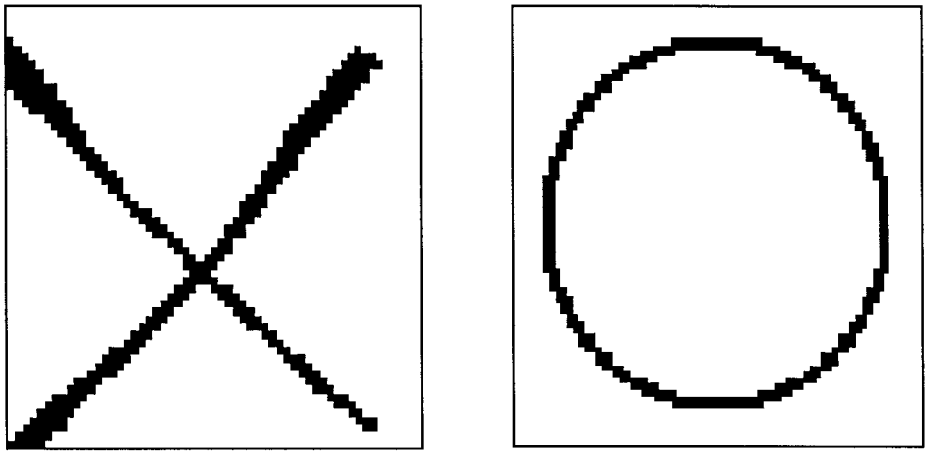

FIG. 1. Perceptual grouping by good continuation. The cross in (a) will be segmented as two intersecting lines on the principle of good continuation. The circle in (b) has good continuation as a whole.

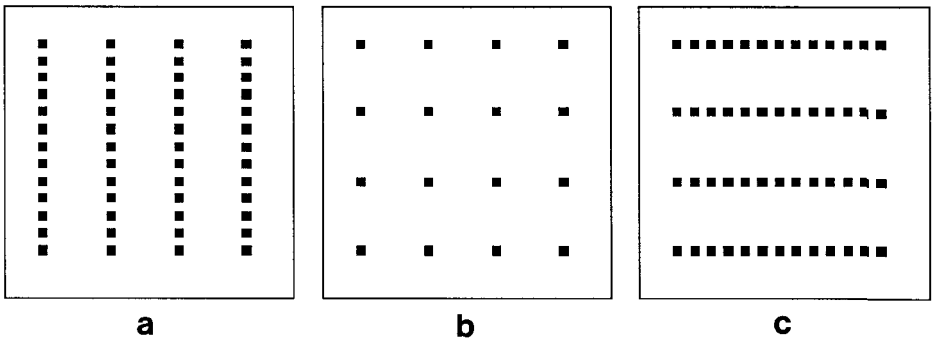

FIG. 2. According to proximity, the array of dark squares in (a) will be grouped vertically and the ones in (c) horizontally. The ones in (b) will be ambiguous with respect to either grouping.

small rectangles are perceptually grouped along the vertical direction; in Fig. 2c along the horizontal direction, according to the law of proximity. Figure 2b is an ambiguous figure. It has multiple interpretations such as a horizontal, vertical, or diagonal groupings of the rectangles (Attneave, 1971) and one interpretation can rapidly switch to another. When these alternative percepts are possible, the system will switch between them on the basis of intermittency.

STABILITY AND INTERMITTENCY IN COUPLED LOGISTIC MAPS

The combination of divergence on some dimension of system behavior and convergence on another is a necessary condition of chaos in continuous systems. In combination with this requirement, some form of periodic behavior is needed which folds the divergent system back to the neighbourhood of the saddle point. Divergence, convergence, and folding behavior must be realized in different subspaces of the system, which implies that for continuous systems, chaos requires at least three dimensions in an Euclidean space. This is not the case for discrete-time systems. A discrete-time system can be obtained from a continuous-time system, for instance by taking a Poincaré section (Norton, 1995), yielding the return map of a discrete system. Such a procedure involves a reduction of dimensions, so the resulting discrete-time system may show chaotic behavior on a single dimension, which exhibits divergence, convergence, and folding.

The logistic map g (Eq. (1) with $0 \leqslant x \leqslant 1$ and $0 \leqslant A \leqslant 4$) is an example of a discrete-time dynamic system meeting

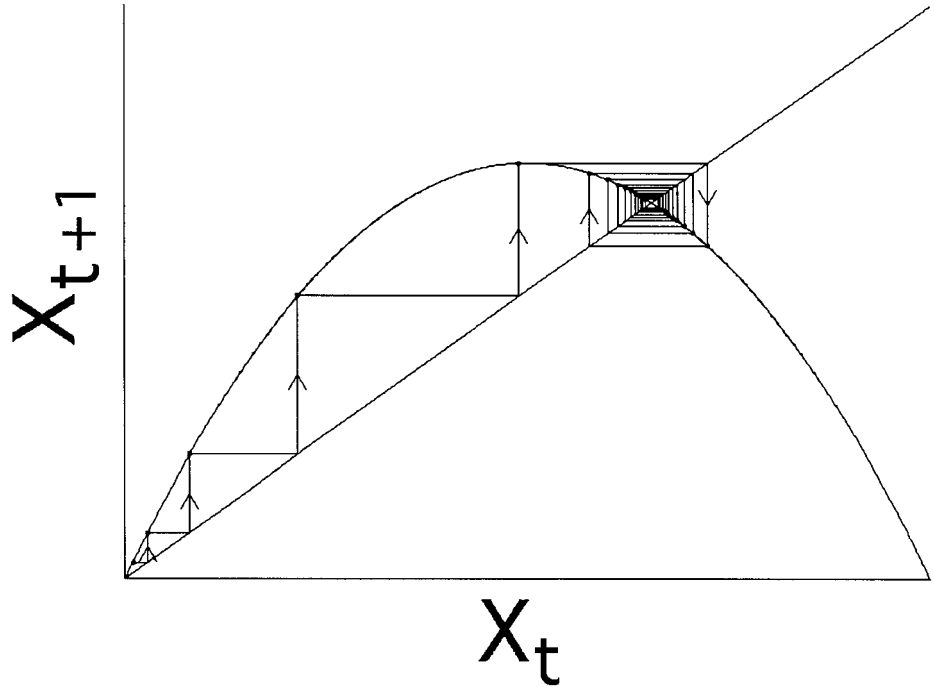

FIG. 3. Progression to a point attractor represented graphically by means of a return map.

this requirement. The logistic map is chosen for our model as a representative family of homeomorphic nonlinear maps (Feigenbaum, 1979). All these maps show a familiar pattern of stability behavior called the period-doubling route to chaos. The system has stationary, periodic, and chaotic attractors, depending on one control parameter (A). Because this behavior is generic, the choice of this particular map within the family is not essential. By using the logistic map, we are, therefore, not implying commitment to the view that neuron firing is the result of a population dynamics, although the present approach does not exclude this either:

$$x^{(1)} = g(x) \equiv Ax(1-x). \tag{1}$$

If $A < 1$ then $Ax(1-x) < x$ and the system will approach zero; if $A \geqslant 1$ and $A \leqslant 3$, g will progress to a constant size depending only on A for all initial conditions x_0 (except for $x_0 = 0$ or $x_0 = 1$). This is shown in the return map of g, where $x^{(1)}$ of g with $A = 2.9$ is plotted as a function of x (Fig. 3). The 45° axis is a useful graphic tool. The cross section with g yields the static point of g, where $x^{(1)} = x$. Iteration of g can be visualized as going from x vertically to the parabola, then horizontally to the 45° axis and from there vertically to the point of interception with the parabola. Repeatedly doing so brings the new values successively closer to the point of interception with the parabola. The static point is therefore an attractor.

A higher value of A will increase the slope of the parabola in Fig. 3. As a result, at $A = 3$, the static point is no longer an attractor. Whereas the static point looses its stability, two stable points are found in the *second-order* return map of g, which plots $g(g(x))$ as a function of x. This plot yields a two-peaked, fourth-order polynomial, crossing the 45° axis in three points. Two of the static points of $g(g(x))$ are stable and accordingly, $g(x)$ will now approach a stable state in which it oscillates with period 2 between these points. This change in the stability of $g(x)$ as a function of A is called a period-doubling bifurcation. It can be observed in the well-known *bifurcation diagram* of $g(x)$ (Fig. 4). Still higher values of A will result in further period-doubling bifurcations, until chaos arises.

The Lyapunov exponent, λ_x of the logistic map is given in Eq. (2). A positive Lyapunov indicates divergence of two signals that start out with infinitesimally small differences. A positive Lyapunov exponent is therefore a necessary condition to call the behavior of a system chaotic. The Lyapunov exponent is a measure for the stability of the attractor:

$$\lambda_x = \lim_{k \to \infty} \frac{1}{k} \sum_{i=t_0}^{k} \ln |A(2x^{(i)} - 1)|. \tag{2}$$

In the lower half of Fig. 4, the Lyapunov exponent is plotted against the parameter A. According to this criterion, for values of A higher than 3.7, the logistic map yields chaotic activity most of the time, except in small bands of periodic activity. These are shown as negative peaks in the Lyapunov function. These negative peaks are known as Arnol'd tongues. In one of the higher Arnol'd tongues, as can be shown in Fig. 4, a cycle of period 3 occurs appears at $A = 3.8282$. The period 3 could be understood from the third-order return map of g, which plots $x^{(3)} = g(g(g(x)))$ against x. This plot has three stable points, one of which does not intersect but *touches* the 45° line.

Just below the value of A, where the function almost touches the 45° line, the dynamic is completely different. The transition is called a tangent bifurcation. For values of A just below the tangent bifurcation, *intermittency* occurs. In Fig. 5, the situation is shown which occurs just before the $x^{(1)} = x$ axis is touched. The trajectory of the dynamic system squeezes through a narrow tunnel between the map and the 45° line. The closer the function is to the $x^{(1)} = x$ axis, the longer on average the trajectory remains in the tunnel. To restrict the operation of our models to a range of A-values within which intermittency could occur, in all simulations A-values will be used between a lower bound, $A_{\min} = 3.7$ and an upper bound $A_{\max} = 4$.

In the presently proposed model, the logistic map (Eq. (1)) is used as local activation function in a neural network of coupled units, because it assures richer dynamics than those of standard connectionist models. It is to be expected that a network of coupled logistic maps will also be capable of stably stationary or periodic activity, as well as chaotic and intermittent behavior. A system of two coupled logistic maps is introduced in Eqs. (3)–(8). The parameter C represents coupling strength; the parameter A, like before, controls the slope of the function; the state variables are x and y, the activities of the two nodes at time t. The variables *netx* and *nety* in Eqs. (3)–(6) are intermediate variables reminiscent of connectionist models. The variables *netx* and *nety* represent net-inputs for the two nodes. Equations (7) and (8) provide alternative coordinates for describing the behavior of the system. Description along the difference (d) and sum (s) coordinate is helpful for characterizing the behavior of the system. For instance, since chaotic activation functions have no stable phase spectrum, synchrony is described in terms of the difference d being reduced to zero. In that case the system will evolve according to the logistic map in the s coordinate:

$$netx = Cy + (1-C)\,x \tag{3}$$

$$nety = Cx + (1-C)\,y \tag{4}$$

$$x^{(1)} = A\,netx(1-netx) \tag{5}$$

$$y^{(1)} = A\,nety(1-nety) \tag{6}$$

$$d = x - y \tag{7}$$

$$s = 1/2(x+y). \tag{8}$$

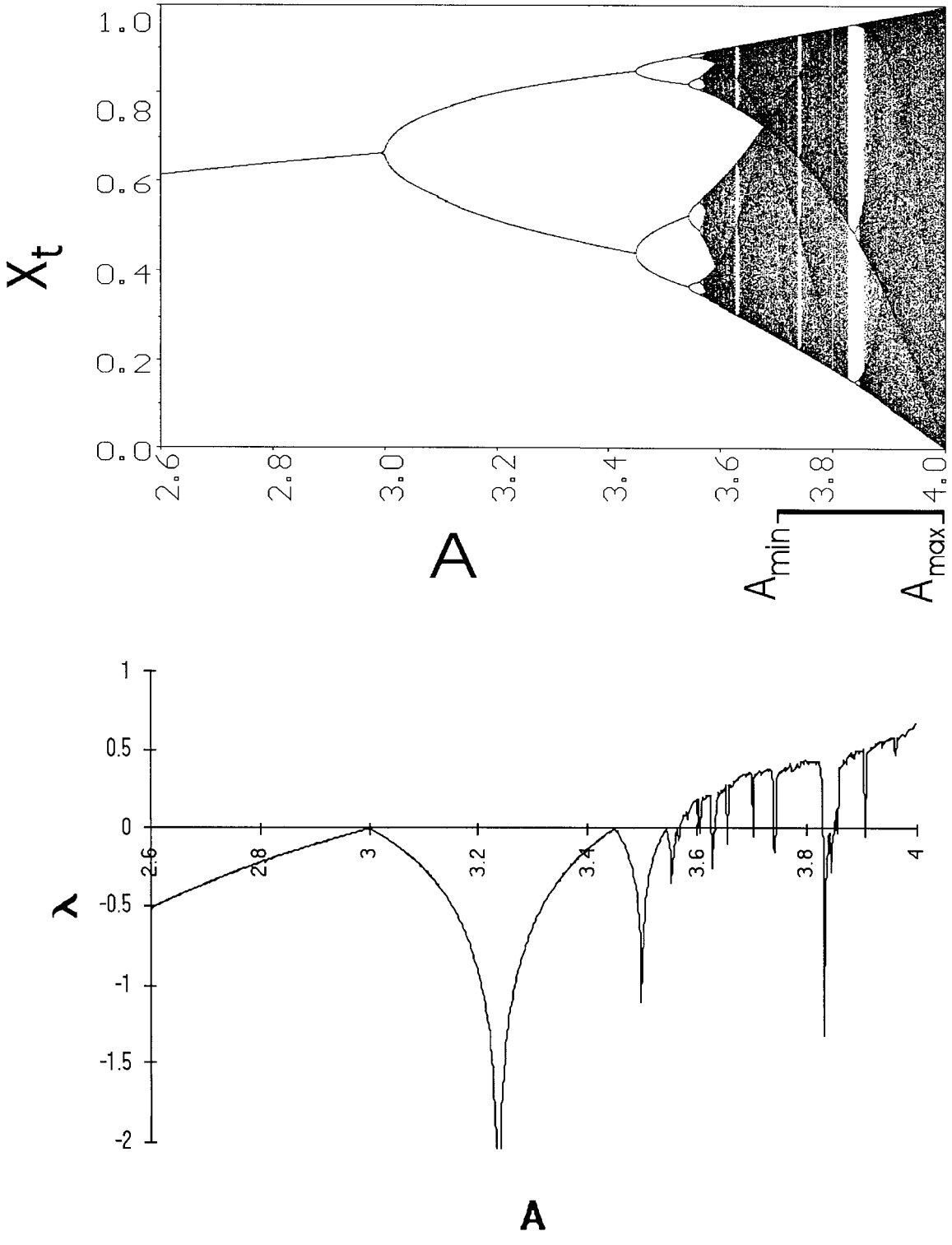

FIG. 4. Bifurcation diagram of the logistic equation (a). Limit values of x are plotted on against the A parameter in the 2.6–4 range. Period-doubling leads to chaos. A_{min} and A_{max} denote the lower and upper bounds of A parameter values used in numerical simulations. In (b), the Lyapunov exponent is shown for the A-values ranging from 2.6 to 4.

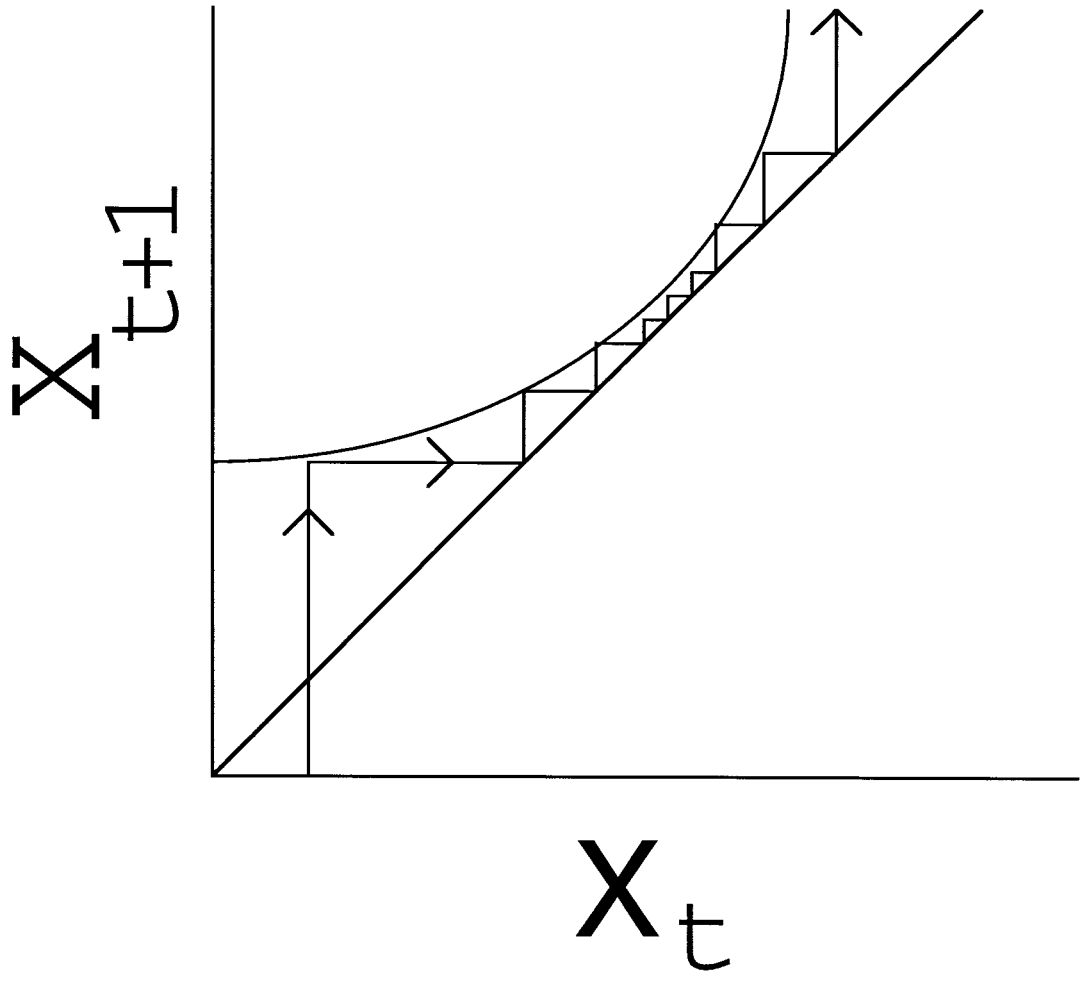

FIG. 5. Intermittency. See text for explanation.

Weights were chosen to be symmetric. This is not an essential feature of the model. However, asymmetric weights can be another source of chaotic oscillation than the one presently under study (Hopfield, 1982). The investigation was therefore restricted to symmetrical weights.

Whereas models to be used in the simulations of perceptual segmentation will be of larger size, the model of Eqs. (3)–(8) consists of only two nodes. A two-node model is the highest level of abstraction for which stable and unstable couplings can be studied. The time characteristics of perceptual stability and state oscillations can already be found in this 2-node deterministic model. If only the timing of the behavior is considered relevant, as in Kelso (1995), this simple version of the model could be considered sufficient. The two-node version is therefore introduced before proceeding to arbitrary-sized coupled nets which are used for simulating perceptual segmentation.

The subsequently proposed segmentation model will operate according to adaptive binding of local input fields. In order to use coupled maps of the type described in Eqs. (3)–(8) in a perceptual segmentation model, two requirements have to be fulfilled: a mechanism for input and one for adaptative coupling between units have to be defined. The coupled logistic maps will provide a convenient way to meet these two requirements. As will be discussed in later sections, the value of control parameter of local oscillation A will come to depend on the local input field. Local input will reduce the rate of chaotic divergence in the model, with the result that the local field is more likely to couple its activity with each neighbour. Hence the function of input is to induce coupling behavior, rather than the propagation of an isolated signal, or feature.

In order to have the system selectively respond to the occurrence of such local coupling tendencies, coupling strength is made adaptive to the coherence in the signal. To fulfil this function, the value of connectivity local parameters C will be used as adaptive weights. The requirements for adaptive binding being fulfilled, the model will be applied to the elementary problems of perceptual segmentation and perceptual switching.

Several studies provide the essential mathematical background for our present adaptive coupling study. The dynamics

of the system as described in Eqs. (3)–(8) is closely related to coupled maps studies found in the literature (Gu *et al.*, 1984; Hogg & Huberman, 1984; Kaneko, 1983, 1984; Schult *et al.*, 1987; Waller & Kapral, 1984; Yamada & Fujisaka, 1983). In these studies, however, the coupling term is linear. The nonlinear coupling term chosen for the present model has been pioneered by Kaneko (1989, 1990) who, through numerical studies, explored the stability characteristics of systems with a range of fixed and uniform A and C values for a variety of network structures and sizes. Numerical solutions in general were shown to be structurally stable. In the following sections, analytic and numerical methods are presented for studying convergence to synchrony. Monotonic and long-run convergence are distinguished.

MONOTONIC CONVERGENCE

For certain critical C_{crit} values of C, $|d|$ decreases at every time step. Finding monotonic convergence is straightforward. Inserting Eqs. (3) and (4) into (5) and (6) we get:

$$x^{(1)} = A[(1-C)\,x + Cy][1-((1-C)\,x + Cy)] \tag{9}$$

$$y^{(1)} = A[(1-C)\,y + Cx][1-((1-C)\,y + Cx)]. \tag{10}$$

It is helpful to express x and y in terms of difference and sum coordinates. Subtracting Eq. (10) from (9) we get, after some algebra:

$$x^{(1)} - y^{(1)} = A(1-2C)(x+y-1)(x-y), \quad \text{or}$$

$$d^{(1)} = A(1-2C)(2s-1)\,d. \tag{11}$$

As x and y are bound between 0 and 1, the value of $|(2s-1)|$ will always be smaller than 1. Therefore, $d^{(1)}$ will always be smaller than d under the condition that $|A(1-2C)| < 1$. In other words, for $1/2(1-1/A) < C < 1/2(1+1/A)$, the difference between the nodes will show a monotonic decrease to zero. This suggests that the proportion of A and C could be used to control stabilization. By choosing an appropriate value of C, large enough to compensate for any chaos tendencies induced by the value of A, stability could be attained in the difference coordinate, even when A prescribes a chaotic regime to x and y.

LONG-RUN CONVERGENCE

In Fig. 6, values C_{crit} of C that lead to convergence in numerical simulations are plotted against A for different initial conditions. The relation between C and A is no longer strictly monotonic. In addition, the value for which synchronicity is observed depends on initial conditions. A correlation between C and A is still preserved. For instance for $A = 3.7$, $C_{\text{crit}} = 0.15$, for $A = 4$, $C_{\text{crit}} = 0.25$. Similar results were reported by Kaneko (1989, 1990).

Values of A and C for which long-run convergence can be obtained are ones for which the coupled state is an attractor.

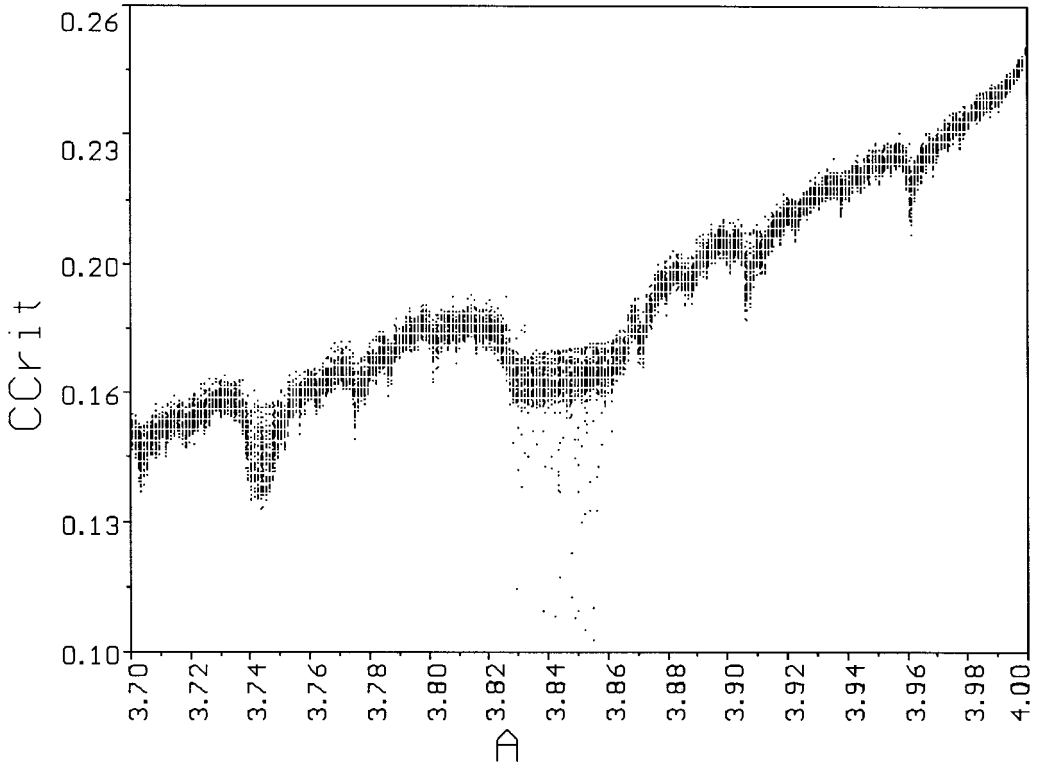

FIG. 6. Plot of C_{crit} (value of C required for synchronization) versus A for random initial conditions in numerical simulations.

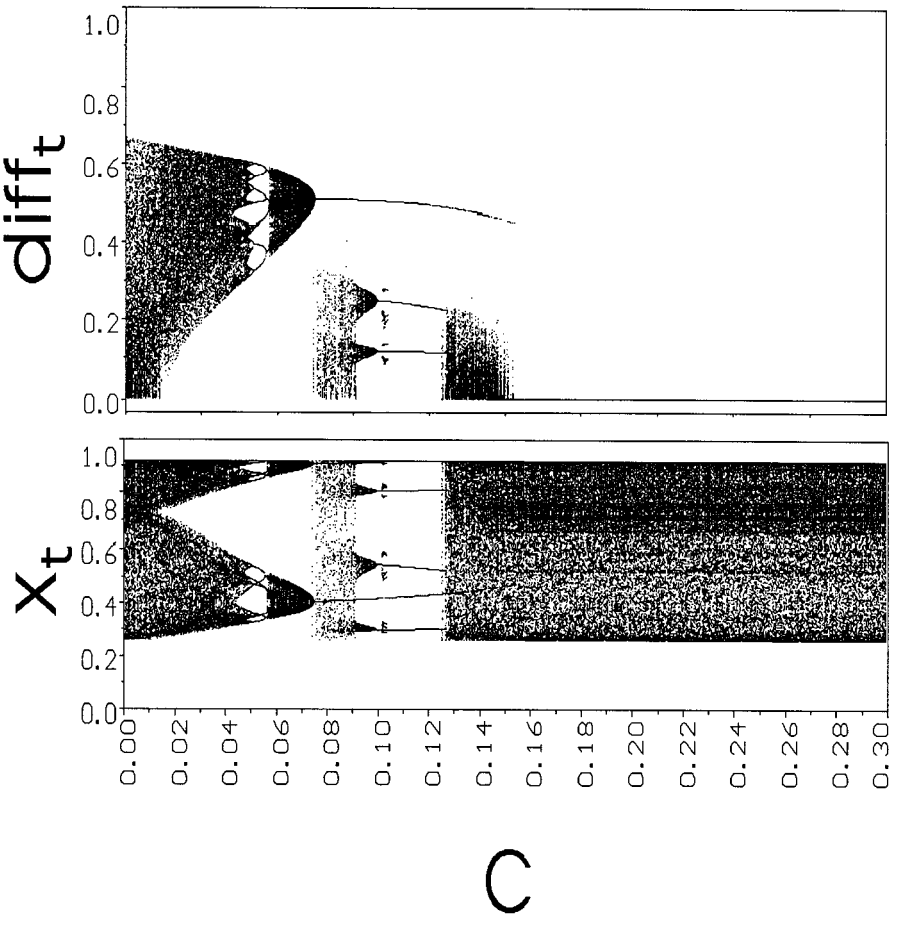

FIG. 7. The effect of the coupling parameter on the synchrony of two nodes when $A = A_{\min}$. The upper graph shows the measure for synchrony diff, the lower one activity x, both versus coupling strength C. For values of C above the critical value C_{crit} there is perfect synchrony indicated by diff $= 0$ and chaotic activity in x. Below C_{crit} periodic and quasiperiodic behavior, and crises can be observed in diff as well as in x.

This implies that if behavior is restricted to the d coordinate, $d = 0$ must be a fixed point. We observe from Eq. (11) that the difference d after two time steps is as in Eq. (12a) and in general for k time steps as in Eq. (12b).

$$d^{(2)} = A(1-2C)(2s^{(1)}-1)\,d^{(1)} = A^2(1-2C)^2\,(2s-1)(2s^{(1)}-1)\,d, \tag{12a}$$

$$d^{(k)} = A^k(1-2C)^k \prod_{i=0}^{k-1} (2s^{(i)}-1)\,d. \tag{12b}$$

From Eqs. (12a) and (12b) it is obvious that if d takes on the value zero, $d^{(k)}$ will be zero for any value of k. So $d = 0$ is a fixed point of the system along the d coordinate. The stability of the system for $d = 0$ (whether or not $d = 0$ is an attractor of the system) also depends on the values assumed by the s coordinate. By combining Eqs. (9) and (10) we get Eq. (13) for s.

In order to calculate the stability of the d, s-system at $d = 0$, the *Jacobian* J of the system has to be determined. The Jacobian is defined as the matrix of derivatives in Eq. (14a), where dp/dq denotes the partial derivative of p with respect to q. The Jacobian for the d, s-system is given in Eq. (14b). To find out whether $d = 0$ is an attractor, the eigenvalues of the Jacobian have to be calculated. The eigenvalues represent the rates of expansion or contraction along orthogonal dimensions. Stability requires contraction, i.e., an eigenvalue less than 1. For $d = 0$, J becomes diagonal. The eigenvalues then equal the multipliers of s and d, which can be obtained directly from the diagonals. The multiplier of s is given in Eq. (14c) and that of d in Eq. (14d):

$$s^{(1)} = A(s - s^2 - 1/4d^2(1-2C)^2) \tag{13}$$

$$J = \begin{pmatrix} \dfrac{ds^{(1)}}{ds} & \dfrac{ds^{(1)}}{dd} \\ \dfrac{dd^{(1)}}{ds} & \dfrac{dd^{(1)}}{dd} \end{pmatrix} \tag{14a}$$

$$J = \begin{pmatrix} A(1-2s) & 1/2Ad(1-2C)^2 \\ 2A(1-2C)\,d & A(1-2C)(1-2s) \end{pmatrix} \tag{14b}$$

$$\mu_s = \lim_{k\to\infty} \prod_{i=t_0}^{k} |A(1-2s^{(i)})|^{1/k}$$

$$= \lim_{k\to\infty} e^{[(1/k)\sum_{i=t_0}^{k} \ln |A(2s^{(i)}-1)|]} = e^{\lambda_s} \tag{14c}$$

$$\mu_d = \lim_{k\to\infty} \left[\left| (1-2C)^k \prod_{i=t_0}^{k} A(1-2s^{(i)}) \right| \right]^{1/k}$$

$$= |(1-2C)| \lim_{k\to\infty} e^{[(1/k)\sum_{i=t_0}^{k} \ln |A(2s^{(i)}-1)|]}$$

$$= |(1-2C)|\, e^{\lambda_s}. \tag{14d}$$

The λ_s in Eq. (14c) is identical to the Lyapunov exponent for the single logistic map as defined by Eq. (2). In general, there is a simple relation between multipliers and Lyapunov exponents: $\mu = e^{\lambda}$; a multiplier smaller than one corresponds to a negative Lyapunov exponent; both divergence and Lyapunov exponent indicate whether a fixed point is an attractor. The value of λ_s is well known. For $A = 4$, $\lambda_s = \ln 2$, so $\mu_s = 2$.

The multiplier for d in Eq. (14d) yields convergence for $A = 4$ and $\lambda_s = \ln 2$ if $0.5 > C > 0.25$. This accords to our numerical simulations. Note that stable synchronization is possible, despite the fact that the behavior in the s coordinate can be stationary, periodic, or chaotic, depending on μ_s.

Figures 7 and 9 show two x and d activity graphs; the corresponding Lyapunov exponents are given in Figs. 8 and 10. These Lyapunov exponents were calculated by a procedure adapted from Hogg and Huberman (1984). This procedure is an alternative to the one described above. The Lyapunov exponent, $\lambda_{x,y}$ with initial conditions x and y is obtained numerically according to Eq. (15),

$$\lambda_{x,y} = \lim_{k\to\infty} \{\ln(\|\mathbf{D}^{(k)}(x, y)\|)/k\}, \tag{15}$$

where $\|\mathbf{D}^{(k)}(x, y)\|$ is the norm of the derivative matrix $\mathbf{D}^{(k)}(x, y)$ which can be iteratively calculated by

$$\mathbf{D}^{(k)}(x, y) = \mathbf{D}(x^{(k-1)}, y^{(t-1)}) \cdots \mathbf{D}(x^{(1)}, y^{(1)})\, \mathbf{D}(x, y) \tag{16}$$

and the derivative matrix of the system described by Eqs. (3)–(8) is

$$\mathbf{D}(x, y) = \begin{matrix} \lceil AC(1-2xC-2y+2yC) \\ \lfloor A(1-C-2xC+2yC^2-2x+4xC-2xC^2) \end{matrix}$$
$$\begin{matrix} A(1-C-2xC+2xC^2-2y+4yC-2yC^2) \rceil \\ AC(1-2yC-2x+2xC) \rfloor \end{matrix}. \tag{17}$$

This procedure can easily be generalized to N-sized networks. The norm of an $N \times N$ matrix $\mathbf{D}$ is defined as $\|\mathbf{D}\| = \max_{\{\mathbf{v}\}} \{|\mathbf{D}\mathbf{v}|/|\mathbf{v}|\}$, where vector $\mathbf{v}$ ranges over all nonzero N-vectors.

Figures 7 and 9 compare the effect of increasing the coupling strength C on synchrony for two different values of A. With increasing C, both the chaotic behavior of x and d is reduced to quasiperiodicity. The quasiperiodicity is indicated in Figs. 8 and 10 by the Lyapunov exponents taking zero values. For some initial conditions, these phenomena arise for lower values of C than for others. Quasiperiodicity is not the rule before transition to stability; the behavior before transition can also take the form of (inversed) period doubling bifurcations or crises. At a critical value C_{crit} of C a sudden transition to synchrony occurs.

When synchronized, the individual nodes resume chaotic behavior as can be observed from the x activity graphs and their Lyapunov exponents; when x and y are synchronized, these are positive and both signals x and y are chaotic.

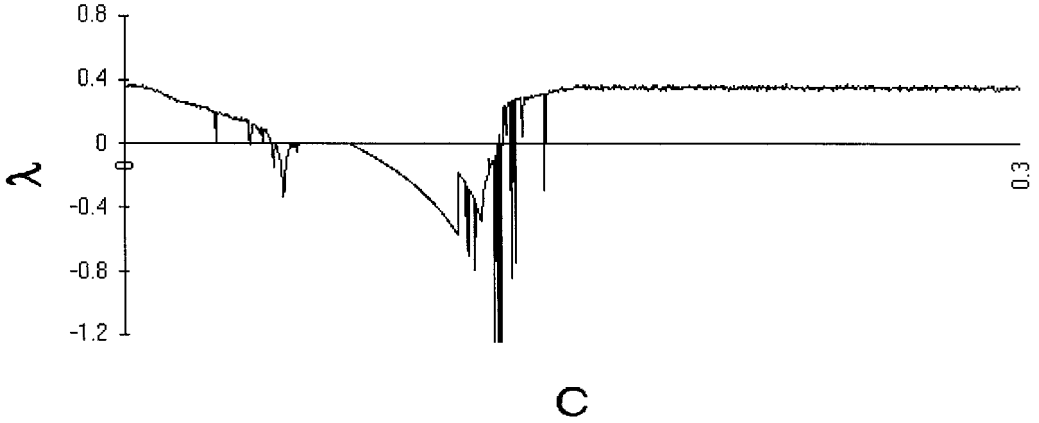

FIG. 8. The Lyapunov exponent versus C for the $A = A_{\min}$. For all C-values greater than C_{crit}, the exponent is positive, indicating chaotic activity. There are windows of stability for values below C_{crit}, which may form obstacles to further synchronization when C is adaptively increased.

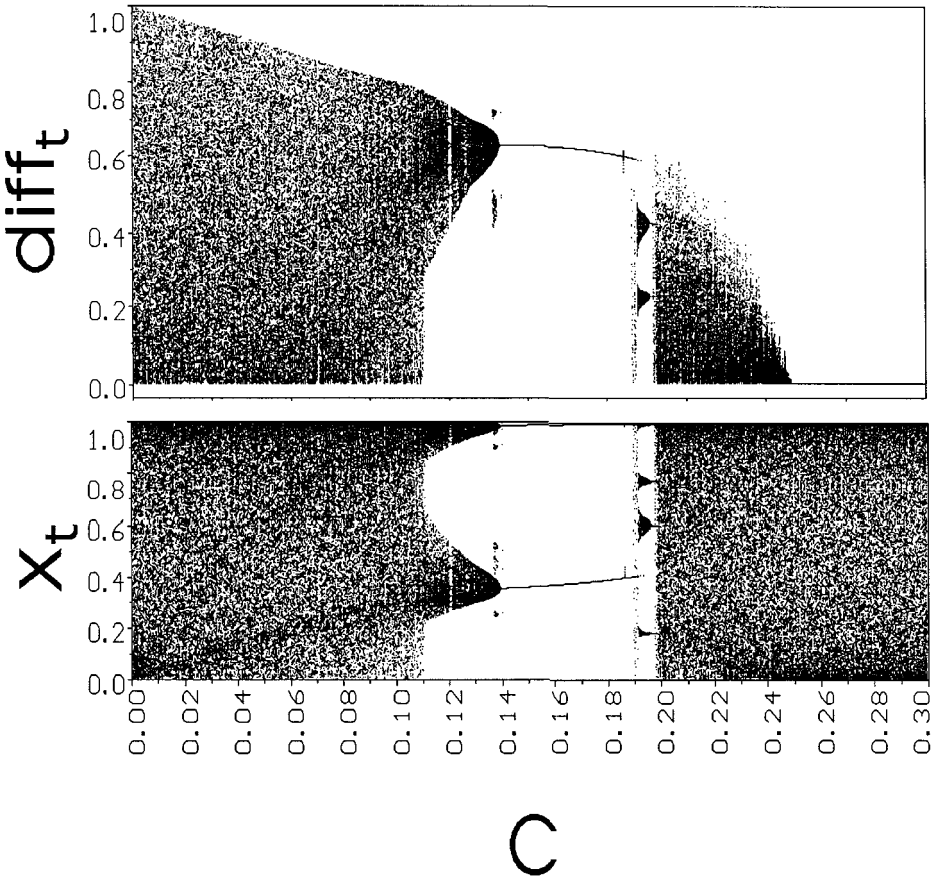

FIG. 9. The effect of the coupling strength on the synchrony of two nodes when $A = A_{\max}$. The upper graph shows synchrony measure diff, the lower activity x, both versus coupling strength C. Full synchronization is reached for a higher value of C.

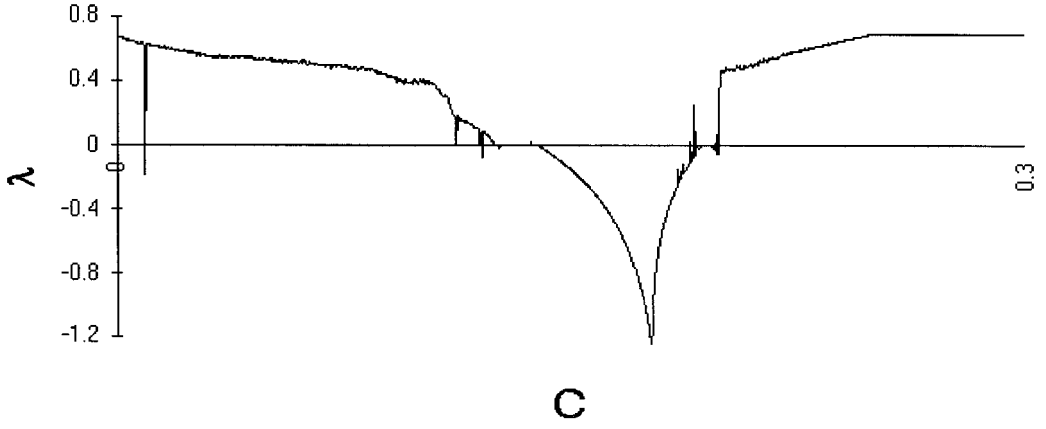

FIG. 10. The Lyapunov exponent vs C for $A = A_{\max}$. For all C-values greater than C_{crit}, the exponent is positive, indicating chaotic activity. The window of stability for values below C_{crit} are more pronounced than in Fig. 8. Adaptive coupling will be less efficient.

N-SIZED FULLY CONNECTED NETWORK

The results on stability in the difference coordinates from the previous section can be generalized to a fully connected network of n nodes. If uniform weights are imposed on the network, like before, the critical value C_{crit} for which full coherence of the network is reached can be calculated from the Jacobian of the system. In analogy to the system of Eqs. (3)–(8) we consider the system of Eqs. (18)–(19):

$$x_i^{(1)} = A net_i(1 - net_i) \tag{18}$$

$$net_i = (1 - C)\, x_i + \frac{C}{N-1} \sum_{j \neq i}^{n} x_j. \tag{19}$$

Note that for larger systems the connections between the nodes become weaker. This is necessary to keep the values of the x_i between 0 and 1. Sum and difference coordinates are defined in analogy to Eqs. (7) and (8) as $s = 1/n \sum x_i$ and $d_i = x_i - x_{i+1}$ for $i < n$, respectively. In terms of these coordinates it can be shown that the Jacobian matrix becomes diagonal when all differences are zero. The Jacobian can be written as

$$J = A(1-2s) \begin{pmatrix} \gamma & & & \\ & \gamma & \phi & \\ & \phi & \cdots & \\ & & & 1 \end{pmatrix} \tag{20}$$

with $\gamma = 1 - NC/(1-C)$. All difference coordinates have eigenvalues $A(1-2s)\,\gamma$, and s has eigenvalue $A(1-2s)$. Like in the two-dimensional case, the synchronization behavior of the system depends on the proportion of A and C. The completely synchronized state is an attractor if $\gamma e^{\lambda_s} < 1$. Dependent on the value of λ_s, the attractor can be a fixed point, periodic or chaotic.

Kaneko (1990) explored the system using a range of uniform values of A and C at or below the level of full synchronization. Below the values of A and C, where full synchronization is reached (coherent phase), the overall organization breaks down into several clusters of synchronized activation. The number of clusters depends on the values of A and C, as well as on the initial values of the nodes. Clusterings are stable under the parametrizations in the ordered phase; yet there are also some parametrization in which glassy, intermittent and turbulent dynamics are encountered as shown in Fig. 11.

The glassy phase is characterized by a degenerate attractor landscape; approach of a stable clustering is frustrated. An intermittent phase is situated between the ordered and the turbulent phase. In this phase, different-sized clusters appear which, however, break down after some interval. In both glassy and intermittent phase, small cluster, or many cluster, solutions are possible, depending on initial conditions.

Also in the ordered phase, the number of clusters in the stable solutions depends on initial values. There is, however, a predominance of few-cluster solutions in case the A and C parameters are chosen near the coherent phase. Near the turbulent phase, many-cluster solutions tend to be more frequent. Yet, few-cluster solutions keep appearing, too.

Kaneko (1990) further observed a correlation between the regularity of the activity within the clusters and two

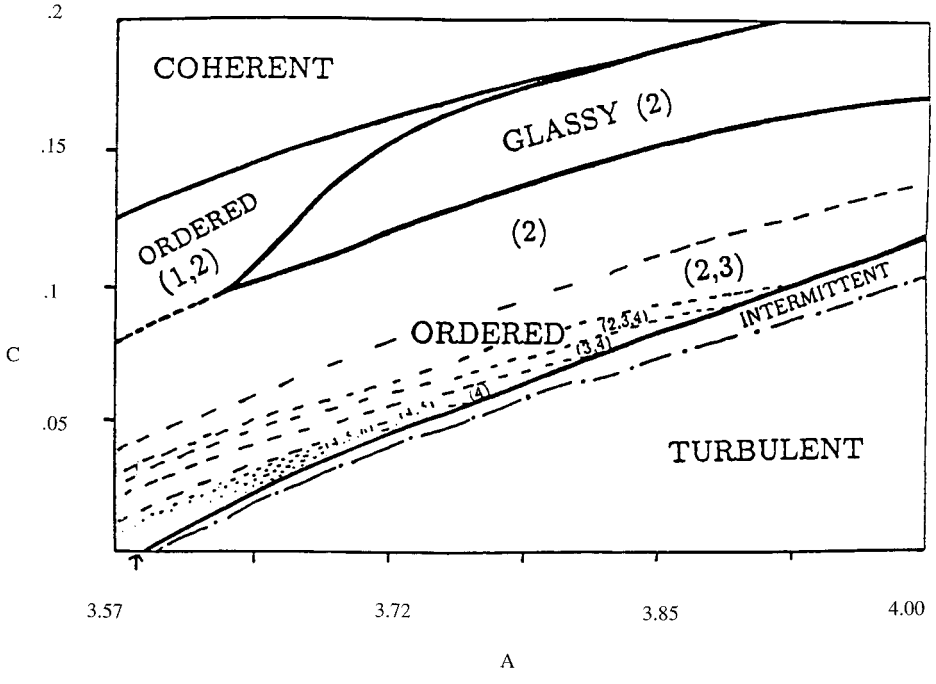

FIG. 11. Exploration of the system dynamics for a fully coupled net (adapted from Kaneko, 1990).

factors, viz. the equality of cluster size and the number of clusters. Regarding the first factor, equality or inequality of cluster size, assume that, for a given combination of C and A, the attractor is a two-cluster solution. With equally sized clusters, two-cluster solutions have a 2-period (or are quasi-periodic in the 2-band). The two clusters oscillate out of phase with each other; the oscillations are symmetrical. If the clusters are unequal in size symmetry is lost. With still larger cluster size inequality, periods double, and with still larger cluster size differences, chaotic activity within the clusters is obtained (quasiperiodic solutions change into chaos directly).

There is only limited tolerance for inequality of cluster size. If the size inequality reaches a critical value, no more stable 2-cluster solutions are possible. The critical value depends on the C and A parameters. The same behavior as with two clusters (stronger suppression of chaos with equal flusters and limited tolerance of cluster size inequality are also obtained with more than two clusters). Altogether, chaos is more effectively suppressed if clusters are large and of equal size.

Controlling the system by adjusting the proportion of C and A, shows a general effect beyond the situation where full synchronization is reached. Increases in C relative to A will lead to fewer clusters, which are more uniform in size, and increased stability. This shows that increasing C in proportion to A can be used to make the system approach a more global state of organization (few large clusters) and reducing C relative to A will produce more local solutions (many small clusters). Thus, nonspecific control on the type of organization (local or global) is possible. This type of control is in accordance experimental observations on strategic control on switching behavior by Peterson and Hochberg (1983), with the theory of attentional processes operating on perceptually segmented regions (van Oeffelen & Vos, 1982) and with the theory of perceptual organization that was proposed by the first author of this article.

When the attractor of the system consists of more than two clusters, there will be larger periods, even if the size of the clusters is (approximately) equal. In general, chaos is less effectively suppressed if the number of clusters is larger; periods are longer and chaos more rapidly emerges. In other words, global organization is more stable, as is in general the case in perceptual organization.

Other aspects of Kaneko's simulations are at least suggestive of psychological applications in the domain of perception. With the 3-cluster attractors, for instance, the system consists of two super-clusters which oscillate out of phase with each other, just as in the 2-cluster case. One of these superclusters is split into two clusters, which oscillate in-phase in the period 2 band, but out of phase in the period-4 band. This illustrates that different clusters of synchronized activity form super-clusters of macroscopically synchronized activity. Kaneko (1990) provides a detailed exposition of these phenomena. Four-cluster and many-cluster attractors are composed in a similarly hierarchical way. This leads to a *hierarchical* composition of the activity patterns; with many clusters a recursive tree structure of higher order superclusters can be found. Thus, the system is capable of expressing hierarchical patterns. This feature of the network is convenient for representations of (perceptual) part–whole hierarchies. The higher order superclusters could be said to be implicit representations of a whole structure.

The considerations about hierarchical composition, combined with those about cluster size as local or global representation, suggest that local solutions (small clusters representing parts of a structure) already contain an implicit representation about the whole. This is why a model using the present one could be said to reach a global structure through self-organization. Synchronization begins from local components; as soon as the local representation is reached, the global one is already implicit. Allowing further synchronization through increases in C or reduction of A values will allow the global representation to become explicit. Thus, the global representation is obtained from the local one in this model through a process of self-organization, or hologenesis (van Leeuwen, in press; van Leeuwen & Bakker, 1995).

LOCAL CONNECTIVITY MODEL

Kaneko (1990) compared the results of numerical simulation for fully connected networks, summarized in Fig. 11, to those of locally connected ones and concluded these to be similar. As before, in the upper-left quadrant of Fig. 11 (low A in combination with high C), coherent states are observed; these are the states where the system tends to synchronize in one single cluster for almost all initial conditions. Ordered states, in which the field develops into clusters of synchronized activity, are possible. Again, chaotic activity is more effectively inhibited with equal-sized and larger clusters. Intermittent and glassy phases also occur in the locally connected,networks.

Kaneko's (1989, 1990) exploration of the rich dynamics of coupled oscillators suggests the possible utility of various possible system states for modelling perceptual segmentation. In particular, the ordered and intermittent states could be used to model stable and ambiguous perceptual segmentations, respectively. In addition, the model meets general theoretical requirements, such as the possibility of nonspecific, strategic control on the growth of synchronized states (van Leeuwen, in press; van Leeuwen & Bakker, 1995). The combination of practical and theoretic utility constitutes sufficient motivation for exploring the potentials of a coupled net of logistic maps as a model of perceptual segmentation. As mentioned, such an application requires an adaptive

algorithm for the coupling parameter C and an input mechanism for the parameter A.

ADAPTIVE COUPLING USING THE C PARAMETER

In the presently proposed model, the uniform fixed coupling parameter is replaced by a set of locally adaptive couplings. In order to do so, Eq. (18) like before specifies x_i as a function of its net input. Equation (19) is replaced by (19′) and Eqs. (21)–(23) are added to the system. As a result, the coupling becomes adaptive to local synchronies in the network. Through adaptation of the c values, a transient synchrony can lead to a stable and lasting one. Two uncoupled chaotic signals are bound to have strong fluctuating differences between them. For some successive time steps, there can be overlap in the activation pattern of the two nodes. resulting in a decreasing difference measure. Then, the weight increases and the coupling increases by which the nodes synchronize more fully and keep synchronized:

$$net_i = \sum_{j \in B(i)} \left(\frac{1 - c_{i,j}}{n-1} \right) x_i + \frac{c_{i,j}}{n-1} x_j \qquad (19')$$

$$diff_{i,j}^{(1)} = |G\, diff_{i,j} + (1-G)\, d_{i,j}| \qquad (21)$$

$$w_{i,j} = 1 - \frac{1}{1 + e^{-H_1(2(diff_{i,j}/H_2)-1)}} \qquad (22)$$

$$c_{i,j} = w_{i,j} C_{\max}. \qquad (23)$$

In Eq. (19′), $n-1$ is the connectivity of the network in the connectivity matrix. In a fully connected network, $n-1$ equals the total number of nodes $N-1$. A function $B(i)$ provides the set of nodes connected to the ith node. As a result of applying Eqs. (21)–(23), the value $c_{i,j}$ of the connection between the ith and the jth node becomes dependent on $d_{i,j}$, the difference in activation value x_i between the ith and the jth node at time t. The intermediate variable *diff* in Eq. (21) is a moving average or leaky integrator of the difference measure d of the two nodes. The parameter G controls the integration rate and has a value between 0 and 1; a low G value results in rapid adjustments to the momentary difference value, a high G to smooth adjustments.

Smoothing was performed because of a particular property of the d values. For instance, in the two-node system of Eqs. (3)–(8), d may reach a fixed point when the two nodes are oscillating in counterphase. Such periodic activity is an obstacle to further synchronization. Counterphase attractors, however, have relatively small basins of attraction and so there are, in principle, two solutions to this problem. One is raising the level of noise in order to drive the system out of the spurious counterphase attractor. The other is attenuation of the spurious attractor state by smoothing. Smoothing is chosen here, because it models one aspect of the behavior of larger locally coupled nets, viz. the delay with which activation from remote nodes arrives. The importance of smoothing, therefore, is expected to decrease for a larger network, more strongly so, since activity from additional neighbours also has a noise function. For locally coupled nets of realistic sizes, smoothing could be omitted fully.

The second intermediate variable, $w_{i,j}$ in Eq. (22), makes the strength of the connection between i and j a sigmoid function between 0 and 1 of this time-integrated difference. The sigmoid is often used without further motivation in connectionism for purposes of producing a step function. Here, it is of importance to notice that this function is 1—a cumulative logistic function. This function is not to be confused with the logistic map which is used as activation function in the present model. By using this sigmoid function, we could be accused of smuggling stochastic assumptions into our model. After all, the logistic function is usually introduced as a probability distribution. However, as we will illustrate with our next simulation, distributions can be obtained with a completely deterministic system, so there is no need to suspect hidden stochastic assumptions in the model. The H_1 and H_2 parameters control the mapping from d to w, where H_1 determines the steepness of the sigmoid and H_2 represents its threshold. H_1 has a function similar to G and H_2's function is similar to that of C; H_1 and H_2 could, therefore, be thought of as redundant. However, we would like to keep the parameters H_1 and H_2, with which semilinear adjustments could be made for tuning purposes, separate from those which have nonlinear influences on system behavior.

Equation (23) scales the connection strengths $c_{i,j}$ to a global parameter $C_{\max}$. In Fig. 12, a value of $C_{\max}$ was chosen for the models so that there can be stable synchrony for $A_{\min}$ and instable and intermittency for $A_{\max}$. A typical time course of *diff* for $A = A_{\min}$ and for $A = A_{\max}$ is illustrated in Fig. 12. This figure consists of two parts. In the upper part, it is shown how stable synchronization is reached after a few iterations for $A = A_{\min}$. In the lower part of the figure, it is shown that with $A = A_{\max}$, a meta-stable synchrony is reached after a few iterations. After the synchrony has been apparently stable for a certain period of time, the synchronization rapidly breaks down and the two nodes resume their independent chaotic behavior.

We may consider the behavior of the two-node system under $A = A_{\max}$ as switching between two alternative states, synchronized versus unsynchronized. If the model is run for an extended period of time, it will go through a sequence of such switches. The interval between two subsequent switches varies considerably in duration. This variation is shown in Fig. 13, which plots the frequency distribution of these periods as a function of their period lengths. The distribution shows a considerable skewness, characteristic of those which are the outcome of a stochastic diffusion process (gamma or ex-gaussian distributions). The present

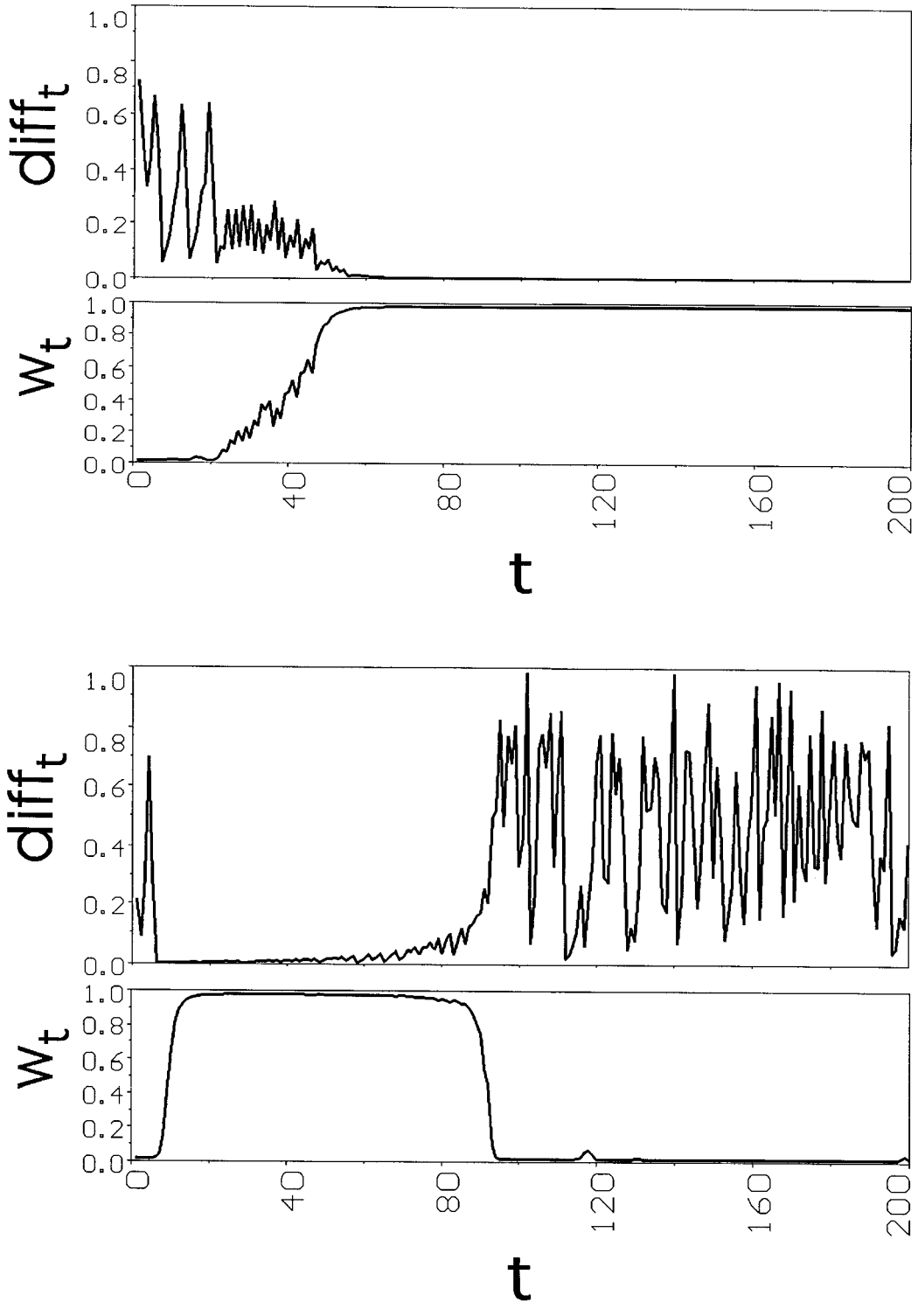

FIG. 12. Effect of A-value on the stability of synchrony in a two-node network with adaptive coupling strength. In (a), $A = A_{\min}$; in (b), $A = A_{\max}$. For both (a) and (b), $H_1 = 5$, $H_2 = 0.3$, $G = 0.8$, and $C_{\max} = 0.24$ and both nodes are started with random initial values. Adaptive coupling yields stable synchronization in (a) and meta-stable synchronization in (b).

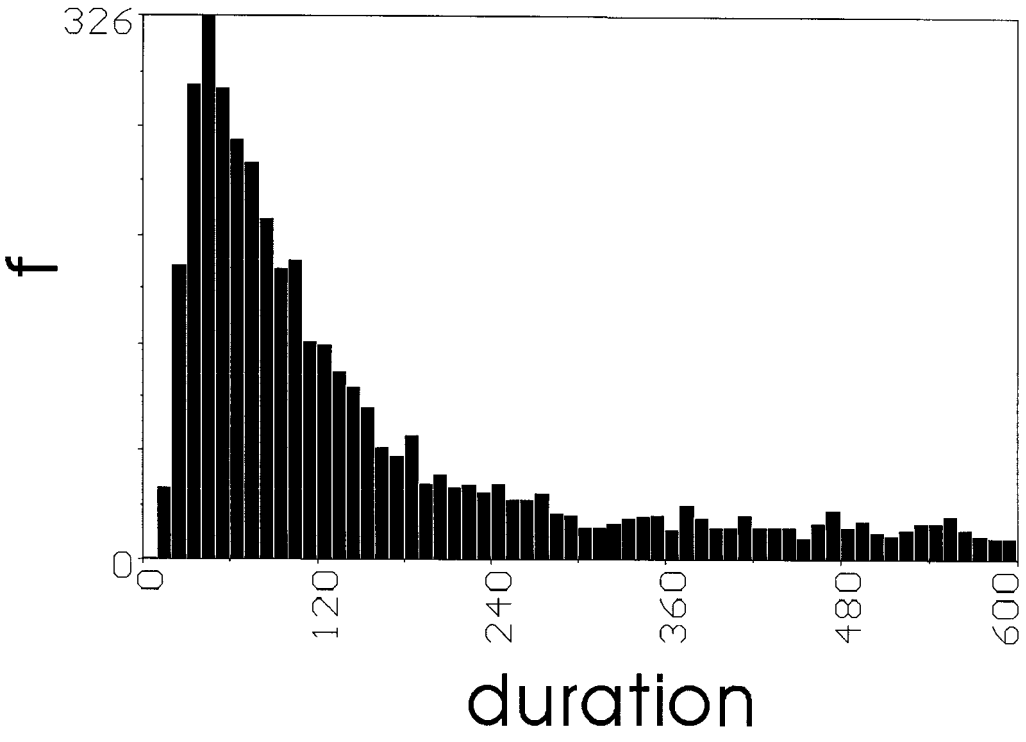

FIG. 13. Frequency distribution of interswitch periods as a function of period length. A switch was defined as the transition from synchrony to no synchrony or vice versa in the two-node model of Fig. 12b with $A = 4$. To calculate a an interswitch period, threshold values on the weight w were assumed. Lower threshold = 0.02, upper threshold = 0.98. The length of the period is calculated as the number of time-steps, w remains above the upper or below the lower threshold. The distribution is drawn for 2,000,000 time-steps sampled with intervals of 10 time-steps.

simulation shows that such distributions can be obtained deterministically.

The parameter $C_{\max}$ determines whether or not the system can reach maximal coherence for random values of x_i in a stable synchrony. If a value of $C_{\max}$ is chosen below the one for which full synchrony is reached, a sufficient degree of coherence between local input fields (see below) will synchronize the system nevertheless. As a result, the parameter $C_{\max}$ can be interpreted as a bias to reach an orderly regime, given the input structure. The comparison between the stability synchrony reached for $A = A_{\min}$ and instability reached for $A = A_{\max}$ suggests that the input function should operate on the A parameter.

AN INPUT FUNCTION OPERATING ON THE A PARAMETER

The next step toward application of the model consists in the specification of its input function. Equation (18′) for $x_i^{(1)}$ replaces Eq. (18). The only difference is that A is replaced by a locally determined A_i, dependent on the input. The present study will concentrate on values of A_i which are independent of time but could easily be extended to the study of time-dependent input patterns $A_i^{(k)}$:

$$x_i^{(1)} = A_i net_i (1 - net_i). \qquad (18')$$

In this section, a system is described which can analyze external input for local spatial frequency features and organize these into a globally coherent topographical map of a pattern. The features of the stimuli are extracted by local oriented spatial frequency analysis using Gabor filters (Daugman, 1985).

Gabor filters can give a complete representation of the input-image, so they do not only have the function of "detecting" oriented features. The filters are operating on overlapping circular receptive fields, each having an origin and a radius that determine the area and the range to which the filter is effective. The receptive fields are equally distributed over the image. The image is expressed as in Eq. (24), which gives the pixel value at the coordinate x_r, y_r relative to the origin of a receptive field.

The filters are sinusoidal plane waves within two-dimensional Gaussian envelopes. The sinusoidal plane wave correlated with the figure is described by Eq. (25), where Ω is the spatial frequency, θ the angle of orientation, and ϕ the phase of the plane wave. The Gaussian is described by Eq. (26), where σ is the standard deviation of the Gaussian that determines the spatial sensitivity of the filter. The complete two-dimensional, phase insensitive Gabor filter is then given in Eq. (27), where $\| \, , \|$ denotes the Euclidian distance:

$$f(x_r, y_r) \tag{24}$$

$$w(\Omega, \theta, x_r, y_r, \phi) = \sin(\Omega(\cos(\theta)\, x_r - \sin(\theta)\, y_r) + \phi)\, f(x_r, y_r) \tag{25}$$

$$g(x_r, y_r) = \exp(-(x_r^2 + y_r^2)/(2\sigma^2)) \tag{26}$$

$$h(\Omega, \theta) = \left\| \sum_{(x_r, y_r)} (w(\Omega, \theta, x_r, y_r, 0)\, g(x_r, y_r), \times \sum_{(x_r, y_r)} (w(\Omega, \theta, x_r, y_r, 1/2\pi)\, g(x_r, y_r)) \right\|. \tag{27}$$

Daugman demonstrated that 2D Gabor filters have optimal joint resolution in that they minimize the product of effective areas occupied in the 2D space and 2D frequency domains. Reducing the standard deviation of the Gaussian, for example, increases the resolution in the spatial domain but decreases its spatial frequency and orientation selectivity.

The function h represents the salience of the orientation feature for a receptive field and is normalized between the rang 0 to 1, where 1 is the maximum value of h for all the filters that are applied. With each receptive field a node i is associated that codes for the feature. The idea is that the salience of a feature determines the control parameter A of the node i, according to Eq. (28), where $A_{\max}$ and $A_{\min}$ determine the range of A-values to which the filter values are mapped. Recall that these A-values are such that the activity in the x_i coordinates would be chaotic in the unsynchronized state:

$$A_i = A_{\max} - h(\Omega, \theta)(A_{\max} - A_{\min}). \tag{28}$$

The more salient the input is to a given receptive field of a node, the lower the A value within the range $A_{\min} - A_{\max}$. Reducing the local A parameter conditionally upon input is in accordance with the proposed control function for this type of model; its effect is a strengthened tendency towards coupling. By an adequate tuning of the parameter space, synchronization near $A_{\min}$, representing the figure, could become stable and near $A_{\max}$, representing the background, would synchronize only temporarily (if at all).

NUMERICAL SIMULATIONS

A locally coupled net was used for the simulations, allowing for a three-dimensional layer-wise representation of a two-dimensional image: the two dimensions of the image in a single layer plus the orientation dimension across layers. Each orientation is associated with a single layer of nodes. If, for instance, the image is analyzed for the four orientations of

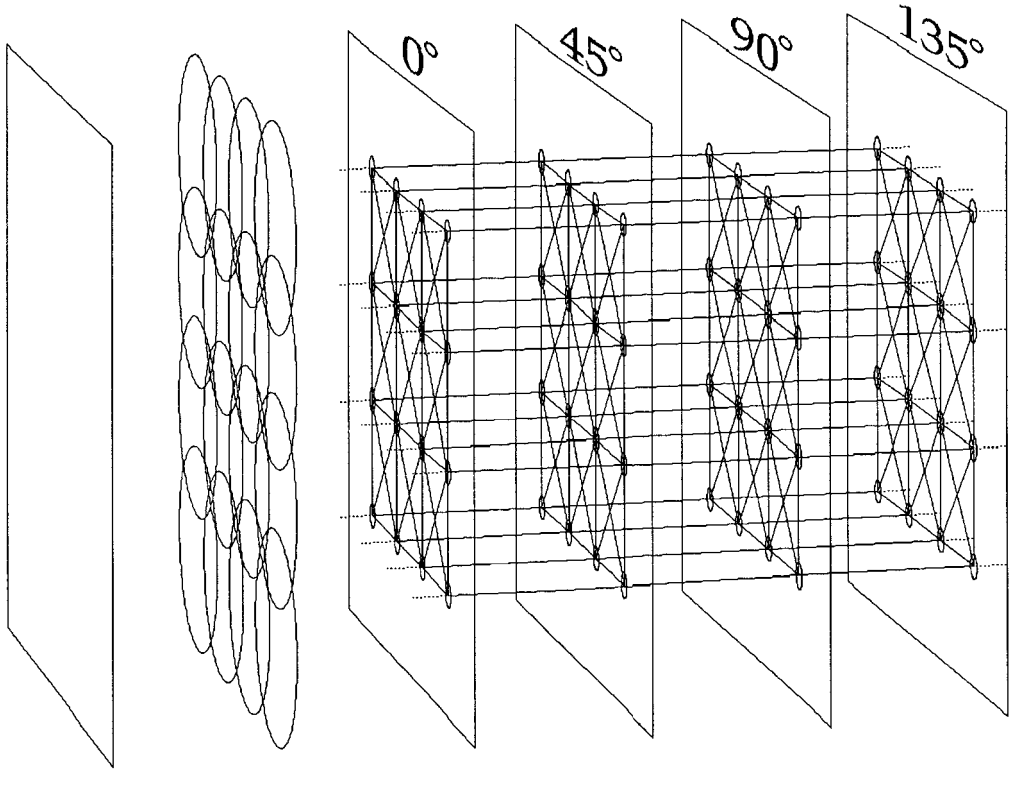

FIG. 14. Typical connectivity pattern within and between layers for a network with four layers for four orientations. Number of nodes within a layer, as well as the number of layers themselves, may vary across simulations. Each node is connected to four neighbours in the same layer and with two neighbours across layers. Nodes at the extremes of each layer are connected to each other and the 0° and 135° orientations are also connected, which implies a hypertorus connectivity structure for the model.

0°, 45°, 90°, and 135°, the model has four layers. Each layer has locally connected nodes which are topographically related to input from the visual field. The nodes are arranged in a grid with N_x and N_y number of nodes with a local connectivity as depicted in Fig. 14. The extremes of the grid are connected to each other, yielding a torus structure for each layer. Eckhorn *et al.* (1990) and Engel *et al.* (1990) have found synchronization between orientation-sensitive layers in visual cortex. The model, therefore, has local connectivity pattern between layers, although there are fewer connections between than within layers. Local connectivity implies that, for instance, the 45° layer is connected to the 0° and 90° layer. The 135° layer is also connected to the 0° layer, sons the whole network has a hypertorus structure. As a result of choosing this structure, boundary problems are avoided.

Numerical simulations were performed on the pattern of two intersecting lines (Fig. 1a) and the circle (Fig. 1b). In all simulations, the weights were initially set to zero. The presence of a signal in the visual field results in a reduction of the A-value of the corresponding nodes, according to Eq. (28). For these nodes, A values were reduced to $A_{\min}$; the others had A near $A_{\max}$. The simulation resulted in the grouping of the intersecting lines as shown in Fig. 15. A connection is shown when its weight $w > 0.7$. The connected nodes in the 45° and 135° layers correspond to line segments of the cross. The grouping obtained by the model is in accordance with the principle of good continuation.

It can be observed that the two diagonal lines are grouped by the layers with diagonal orientation sensitivity (45° and 135°). There are no spurious groupings between the nodes in Fig. 15. These do occur at times, but are transient. Also, the value of w for some of the connections shown in Fig. 15 at times sinks below the criterion level. This is a transient phenomenon as well; the connection is rapidly restored. These fluctuations in the pattern illustrate the effect of chaos revolting against the synchronized pattern. The effect, however, in this case is not strong enough to destroy the pattern and so this pattern is stable.

That only neighboring layers are connected in the model makes, so that whatever changes abruptly in the orientation is likely to be kept separate. Bindings are possible between structures that shift smoothly in orientation across locations the visual field. The circle (Fig. 1b) has gradual orientation differences and should be synchronized by the model as a whole. The result of simulation on the circle pattern is shown in Fig. 16. Connections are shown for $w > 0.7$. As before, any transient groupings are not shown. Since the Gabor filters yield coarse coding of the input, orientation-specific layers will respond to a range of orientations. Grouping is obtained for these nodes, even though for some of them $A > A_{\min}$ as a consequence of coarse coding.

While the grouping develops with time, the pattern undergoes several reorganizations. The synchronization develops from local to global in time. This tendency corresponds to

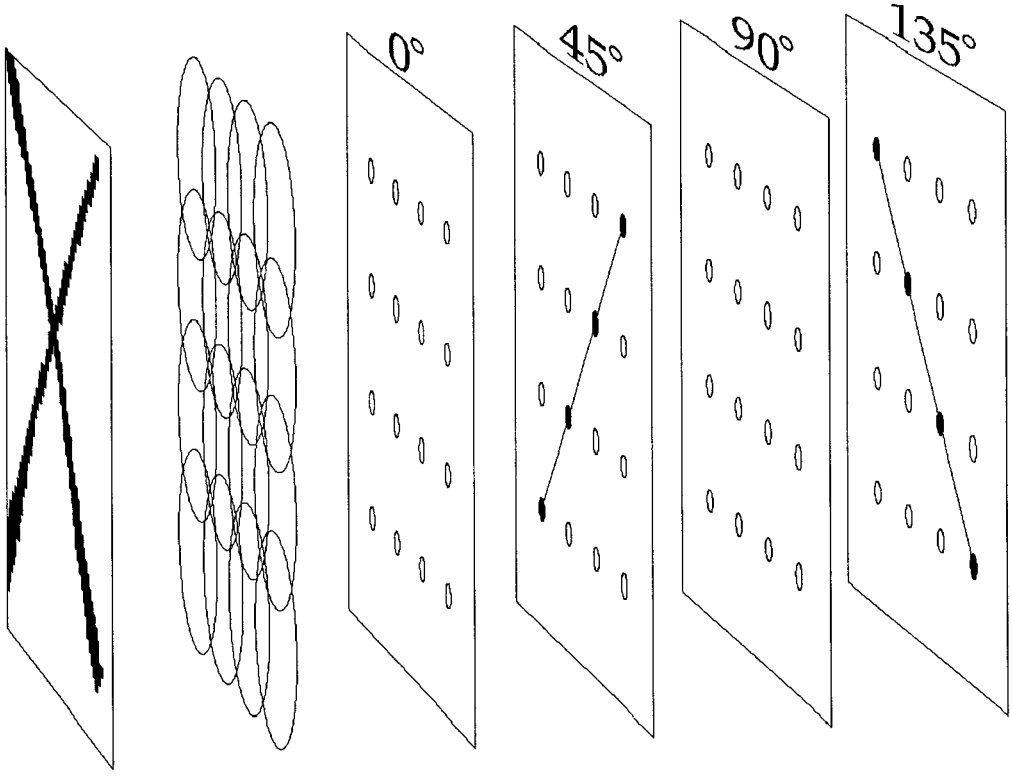

FIG. 15. Grouping obtained from numerical simulation, using the cross (Fig. 1a) as input. The model represents the figure as two intersecting lines. Both lines are desynchronized from each other. The pattern of synchrony is in accordance with the principle of good continuation.

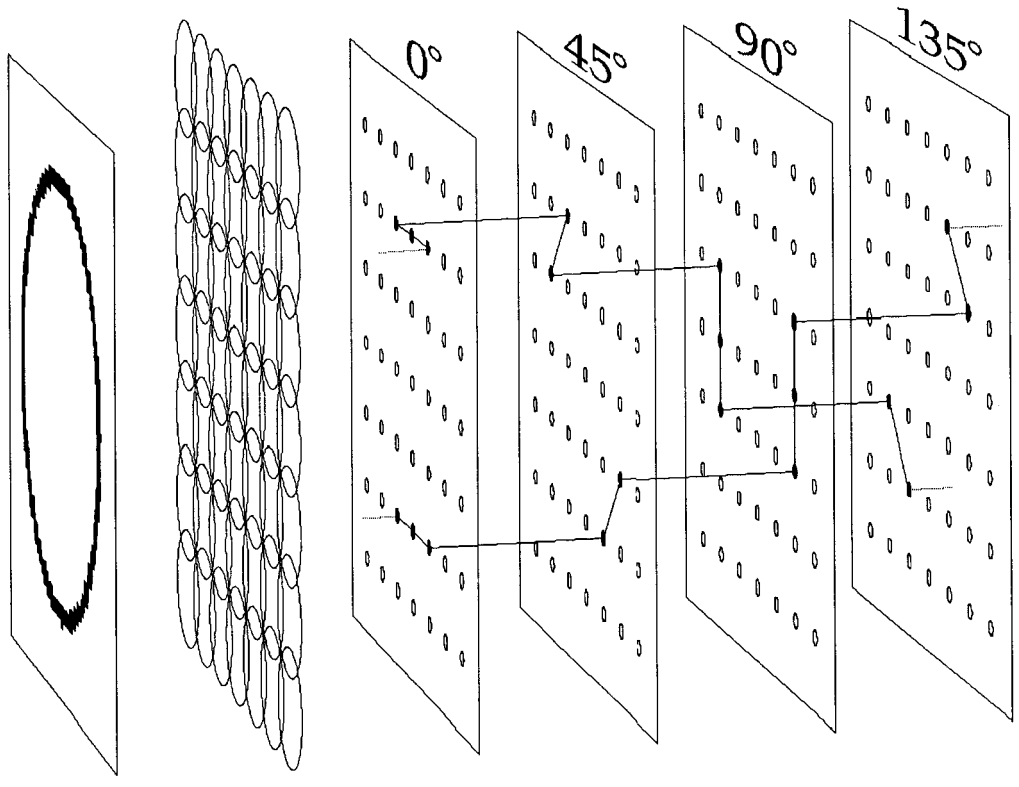

FIG. 16. Grouping obtained from numerical simulation, using the circle (Fig. 1b) as input. The components of the circle are synchronized as a whole. The pattern of synchrony is in accordance with the principle of good continuation.

the principle observed in the growth of perceptually complex structures, called hologenesis (van Leeuwen, in press). Initially there its no grouping. In the next stage there are transient couplings that seem to move along the trajectory of the circle. This phenomenon illustrates that the growth of the percept is nonmonotonic. Then suddenly these transient couplings seem to meet, and stable coupling becomes predominant. Yet there are still gaps: transient, nonsynchronized parts of the circle. Finally the whole circle is completed.

The nonmononicity in the circle example illustrates that, during the self-organizing process of the pattern, perceptual structures could appear which later disappear. This phenomenon is familiar from masking studies. For instance, early during the segmentation process of two occluding squares, a mosaic interpretation is seen (Sekuler & Palmer, 1992). Such nonmonotonicities, which are easy to explain in terms of the present model, are difficult to explain in terms of other approaches, of constructivististic or dynamic breed, to the growth of a percept in the microgenetic time frame tapped by masking studies.

The self-organizing capacity is sufficient to synchronize the circle as a whole. With weaker coupling strength, the circle would have remained a collection of loose segments. With larger values for the coupling strength, or less chaotic divergence, as observed in Fig. 11, there would be uniform synchronization which would have absorbed the circle into its background. The optimal synchronization behavior is found across a range of parameter values, without requiring much fine tuning. With larger and more complex patterns, it will be more difficult to tune the parameters of the system to optimal behavior. In such situations completion of a global structure cannot always be guaranteed, as is shown by the variability in ordered states in Fig. 11. Such constraint on synchronization may lead to a new explanation of spatial attention mechanisms. In this view, restrictions in spatial attention are needed, not in order to reduce computational complexity, but because the resulting patterns will show a great deal of spurious segmentations. This would imply, among others, that the span of spatial attention and the level of perceptual segmentation mutually determine each other and are jointly under strategic control (Hogeboom & van Leeuwen, 1997). This point has been argued independently by others (van Oeffelen & Vos, 1982). The issue of whether these strategic processes could be understood as adaptive self-control is left to later stages of development of the model.

Although the strategic restrictions on synchronization imply that perceptual organization will often be piecemeal (Peterson & Hochberg, 1983), these restrictions should not obstruct the formation of global structure. Usually in neural networks, such structures are the result of automatic generalization, due to the pattern recognition capacities of the

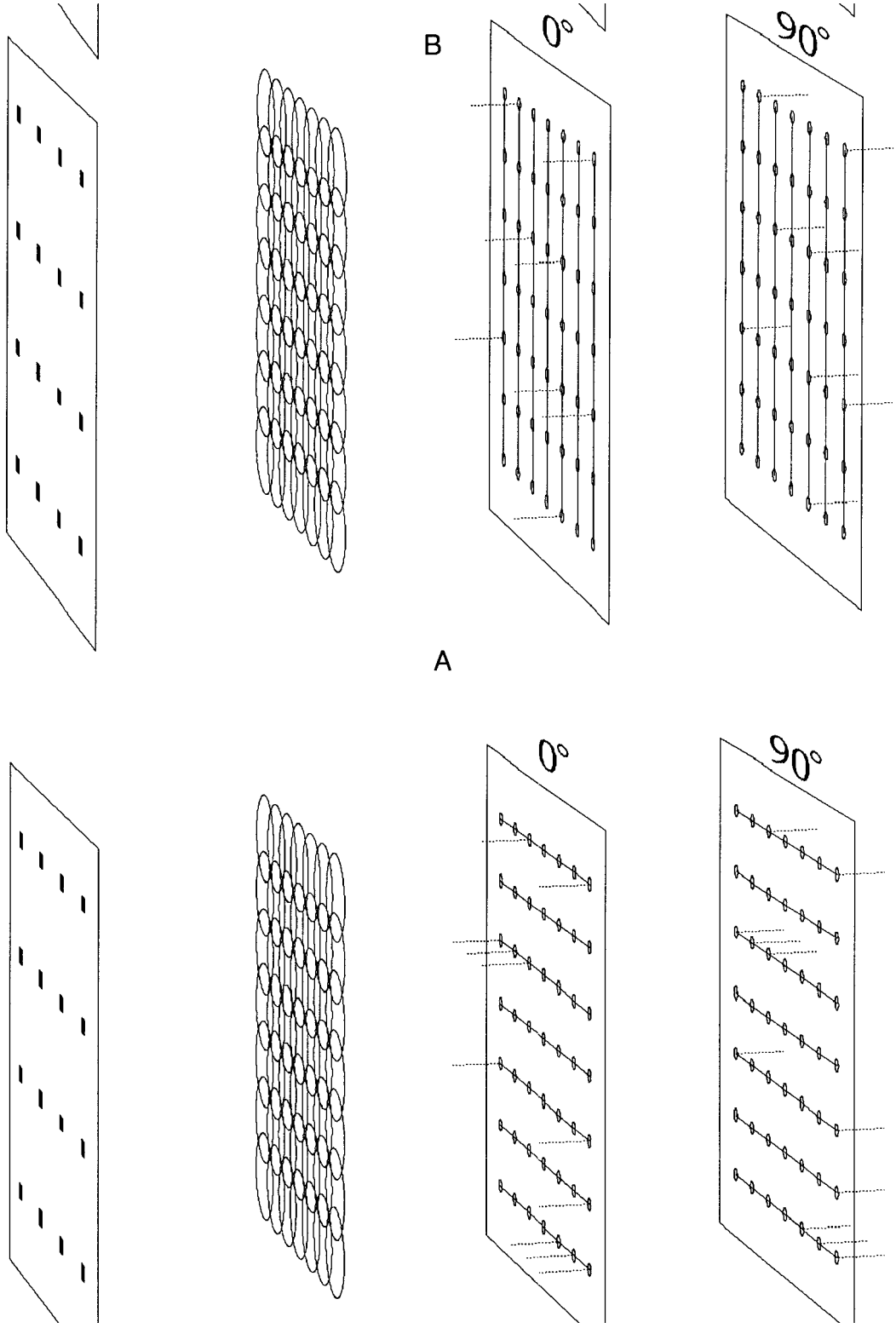

FIG. 17. Groupings obtained from numerical simulation, using the ambiguous pattern of Fig. 2b as input. Alternative groupings occur in the vertical (a) and in the horizontal (b) directions.

adaptive weights. Although the weights in the present model are adaptive, for segmentation purposes the weights adapt at such a fast rate that they hardly have a memory function. As a result, the nodes in the model have no inherent bias for certain connections, e.g., for local symmetries or parallelism of line elements. In later developments of the model, we intend to introduce these biases as an effect of the way the segmentation system interacts with layers of units whose weights adapt at a much slower rate. For the present model we have chosen a provisional solution which models selective facilitation by means of an algorithm.

ALGORITHM 1. (1) for all nodes i at time t, determine the neighbor node k, to which i has the smallest difference $d_{j,i}$ from the set of neighbouring nodes B_i.

(2) label the direction of this connection between node k and i as horizontal, vertical, or as one of the two possible diagonal directions.

(3) for all weights of the nodes n of B_i, alter the weights $w_{j,i}$ by:

$$w_{j,i} = w_{j,i} * S + (1 - S)$$

if direction $m - n$ is the same as $k - i$

$$w_{j,i} = w_{j,i} * S$$

if direction $m - n$ is not the same as $k - i$.

This algorithm gradually increases the weights that lie on the axis of symmetry $k - i$ in the neighborhood of a node (using a moving average with parameter S) and decreases the other, incompatible weights. The algorithm operates on the local neighborhood of every node. Its global effect is to cause the gradual spread of the area of nodes that are synchronized to become biased toward axis-symmetry.

This algorithm was added to the system of Eqs. (18′)–(19′) and applied to the stimuli in Fig. 1. There were two layers, one for the 0° and one for the 90° orientation, each with 7×7 of nodes. For Figs. 2a and c, the system reached a *stable* synchronization in the appropriate layers after approximately 20 iterations. The interesting case is the ambiguous Fig. 2b. For Fig. 2b, there is switching between the horizontal and vertical interpretation, respectively (Fig. 17). Also diagonal interpretations occasionally occur for brief periods. Figure 18 shows a time series for the two major alternative groupings. The switching-time distribution is shown in Fig. 19. A criterion value for horizontal and vertical orientation was calculated by summing for all the horizontal connections and substracting the vertical ones. This criterion was rescaled between 0 and 1. A lower threshold of 0.02 and an upper threshold of 0.98 were set on the criterion. The length of the period is calculated as the number of time-steps, w remains above the upper or below the lower threshold. The resulting distribution is skewed similarly to Fig. 13, which shows a distribution of inter-switch intervals with two coupled nodes. Such distributions are generally thought to be based on stochastic processes in dynamic systems. Here, as in Fig. 13, no stochastic processes whatsoever were involved. The distributions obtained from the model are similar to ones obtained in experimental studies with ambiguous figures (e.g., Borsellino, Carlini, Riani, Tuccio, De Marco, Penengo, & Trabucco, 1982).

In order to obtain Figs. 17 and 18, an external criterion for horizontal or vertical grouping was imposed. The skewness of the distribution in Fig. 19 depends on the upper and lower bounds chosen for this criterion. In other words, the precise fit of experimental data would depend on an arbitrary assumptions. For this reason and because the distribution is irregular, we have to satisfy ourselves with qualitative similarity and no further attempt of calculating an optimal fit to experimental data was made. That the qualitative similarity of this distribution with experimental

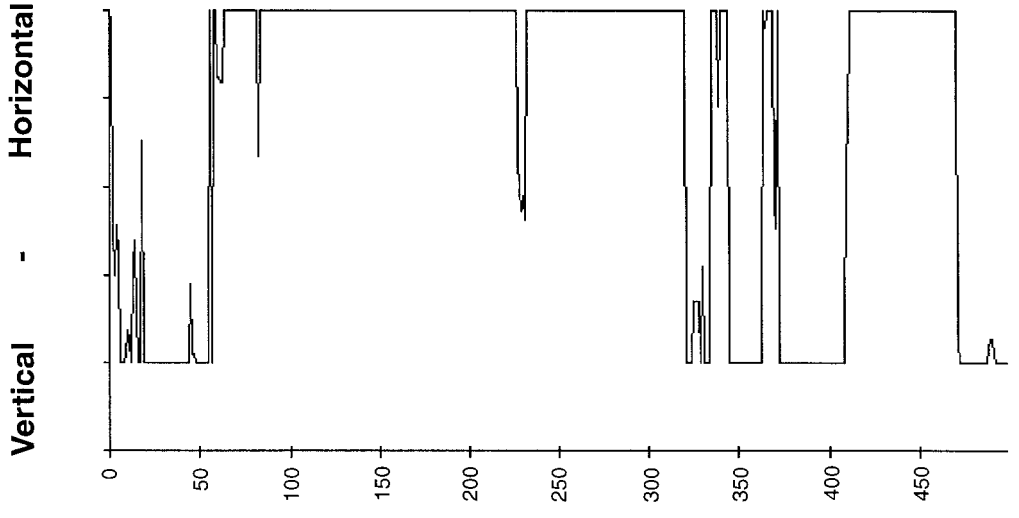

FIG. 18. Switching between vertical and horizontal grouping of the ambiguous pattern in Fig. 2b.

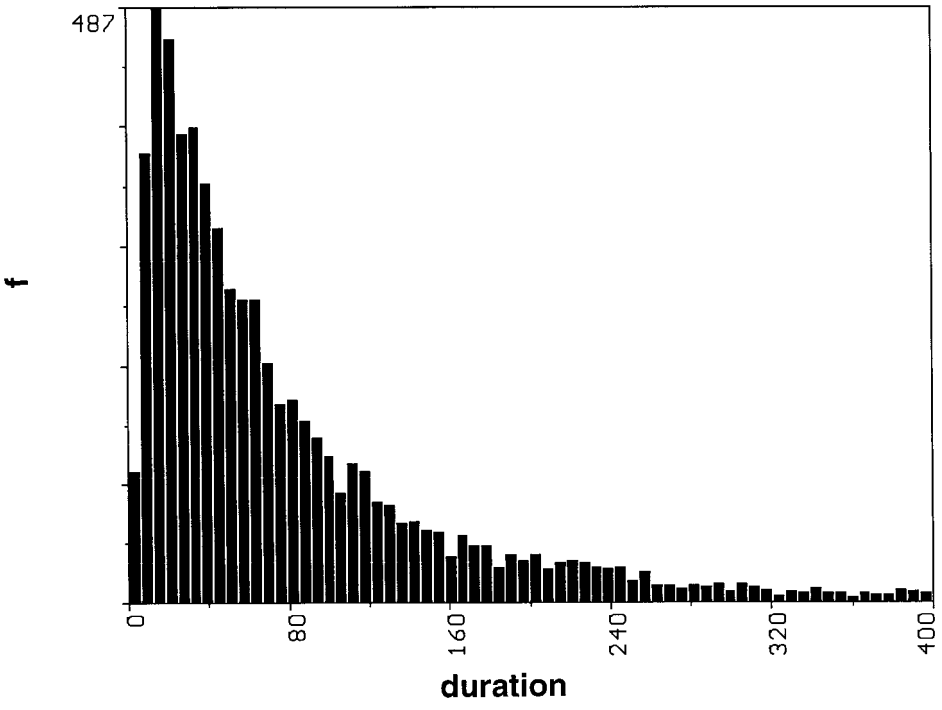

FIG. 19. Frequency distribution of interswitch periods as a function of period length for the ambiguous pattern in Fig. 2b.

data was obtained with only one free parameter ($C_{\max}$), however, is telling.

DISCUSSION AND CONCLUSION

Stable and meta-stable patterns of synchronized activation evolve from high-dimensional, chaotic noise. This principle was used to obtain segmentation of perceptual patterns in a lattice of locally coupled oscillators. The segmentation shown by our model is in accordance with Gestalt principles of proximity and good continuation. For perceptually ambiguous patterns, the system switches back and forth between alternative meta-stable states. The spatio-temporal characteristics of deterministic chaos in activity patterns could thus be brought to bear on the issue of holistic pattern structure.

The growth of pattern structure will begin from the sensory activity of individual receptive fields. Organization occurs through dynamic linking of activity in local populations of neurons. The area of nodes interacting towards segmentation has been called a linking field. According to Eckhorn *et al.* (1990): "These fields were generally found to be much broader than the receptive fields of the nodes." In the model, meaningful synchronization can appear over much broader areas than the size of the receptive field or the area of local connectivity of the node. The model introduces a novel mechanism for modelling the way by which local cortical interactions can induce global activity.

In traditional approaches to neural activity organization, the formation of a meaningful global pattern from the local dynamics requires and relies on the fine-tuning of the units participating in the dynamics. Moreover, each individual unit is conceived to have a precisely defined or at least predictable dynamics. This attitude toward modelling originates in the classical information processing paradigm. For perception, this approach induces an impoverished view on the growth of global structure from the local dynamics of the system. In particular it uses a set of stable, elementary features to build global pattern structure. By contrast, units in the present model are no longer restricted to the sharply defined stability constraints which classical computation would prescribe. Our approach proceeds to a framework which allows all units to have a rich dynamics which is capable of producing a variety of behaviors, including meta-stable and unstable ones. This framework is of particular significance for the construction of perceptual process models from a holistic point of view, since there is no longer a restriction to fixed elementary features.

The enhanced framework allows more realistic modelling of a range of microgenetic phenomena in perception. These phenomena include the self-organization of components organized into a recognizable pattern (Biederman, 1987), the grouping phenomena observed by Sekuler and Palmer (1992), and the time course of eye movements in the visual processing of natural scenes (Henderson, 1992). These phenomena have come within the scope of modelling, because it is now possible to interpret the trajectory towards stability as a perceptual process. Up until now, models emphasized stability and this restricted the significance of trajectories to their final states.

By alleviating the restrictions on the units, the load of explaining the growth of coherence is transferred from control on the units to self-organization. Coherence in the activity of a system is still obtained by modelling the evolution of coupling strengths. However, whereas in classical models the coherence is prefigured by functional requirements on the input representation, in the present model the coherence is conceived as emerging from neural dynamics. Whereas in the classical approach the dynamics subserves an information-processing role, often side-stepping the actual nature of the neural system, in the present approach the self-organization is intrinsic to the system and behaves as if it has information processing significance.

The definition of evolution equations for coupling strength, sufficient to handle chaotic divergence and establish stable segmentation proved relatively simple and straightforward. A restricted set of qualitatively different types of behaviors was observed below the level of coupling strength where full, stable synchronization is reached. In this range of parameter values, spatial and temporal restrictions on synchronization are observed which can be given a straightforward psychological interpretation. Perceptual switching behaviour was obtained in our model for a range of coupling strength values which confined the dynamics of network activity to the intermittent regime.

Different regimes of coupling strength lead to differences in synchronization. Starting from chaotic, irregular behaviour, local linking develops and interacts to form more global structures. When coupling strength is reduced for a given rate of chaotic divergence, linking fields are observed to be relatively small. A range of variation in their size is observed, to the effect that more global organization still is possible with reduced coupling strengths. But on average, larger synchronized are as will be less frequent with smaller values of the coupling parameter. For perceptual patterns, this implies that the pattern cannot be represented as a whole and will remain a collection of separate local components.

Nonspecific control of coupling strength, therefore, has significance for the issue of strategic control in perception. Strategic control on the binding between features and regions, resulting in the processing separate or configural properties (Pomerantz & Garner, 1973; Pomerantz & Pristach, 1989) could now be understood from the spatio-temporal limitations on coherence, of which the control parameter can be adjusted functionally to the task. Individual differences in perceptual style (holistic vs analytic) could be based on the same control dimension.

The present approach implies a view on the relation between controlled and automatic processes that is similar to, but different from, that of Treisman and Gelade (1980). In their view, automatic processing of features is essentially local. Only functionally simple features are processed without attentional effort. Attentional processes integrate these features into a coherent perceptual structure. In the presently proposed approach, automatic processes can yield local features as well as global structure. They do so within the range of an attentional parameter which relates to the level of functional complexity that these global structures can maximally reach, i.e., the number of units that can become synchronized. Strategic control, in other words, is nonspecific. This is in accordance with the view outlined from the onset of this article that the role of strategic control from outside of the system should be minimized.

The basic assumptions of this model with respect to the time course of synchronization and with respect to control may possess significance beyond the time scale of perceptual segmentation. Perceptual comparison experiments reveal a similar time course for classification (Goldstone & Medin, 1994) and perceptual pattern learning (van Leeuwen, Buffart, & van der Vegt, 1988). An interesting development could therefore be to construct a perceptual classification system as a lattice of coupled oscillators, similar to the segmentation system, except for the adaptation rate of the weights, which is much slower for classification than for segmentation.

In further development, two perceptual modules could be assumed to operate in interaction: a perceptual segmentation system and a classification system. The classification system learns from the segmentation system and the segmentation system is corrected by the classification system. A model based on these principles would develop a bias for more stable perceptual organizations in the long run and combine this with flexibility on the short run. The classification system will adapt with preference to the most stable segmentations and, hence, will emphasize regularity in the representation. Such a potentially promising way of implementing a perceptual classification system, with preferences resulting entirely from self-organization, is the long-term goal to which the present model is a first contribution.

REFERENCES

Amit, D. J. (1989). *Modeling brain function*: *The world of attractor neutral networks*. Cambridge, UK: Cambridge Univ. Press.

Attneave, F. (1971). Multistability in perception. *Scientific American*, **225**, 63–71.

Borsellino, A., Carlini, F., Riani, M., Tuccio, M. T., De Marco, A., Penengo, P., & Trabucco, A. (1982). Effects of visual angle on perspective reversal for ambiguous patterns. *Perception*, **11**, 263–273.

Daugman, J. G. (1985). Uncertainty relation for resolution in space, spatial frequency, and orientation optimized by two-dimensional visual cortical filters. *Journal of the Optical Society of America A*, **2**, 1160–1169.

De Marco, A., Penengo, P., Trabucco, A., Borsellino, A., Carlini, F., Riani, M., & Tuccio, M. T. (1977). Stochastic models and fluctuations in reversal time of ambiguous figures. *Perception*, **6**, 645–656.

Ditzinger, T., & Haken, H. (1990a). Oscillations in the perception of ambiguous patterns. *Biological Cybernetics*, **63**, 279–287.

Ditzinger, T., & Haken, H. (1990b). The impact of fluctuations on the recognition of ambiguous patterns. *Biological Cybernetics*, **63**, 453–456.

Eckhorn, R., Reitboeck, H. J., Arndt, M., & Dicke, P. (1990). Feature linking via synchronization among distributed assemblies: Simulations of results from cat visual cortex. *Neural Computation*, **2**, 293–307.

Engel, A. K., König, P., Gray, C. M., & Singer, W. (1990). Stimulus-dependent neuronal oscillations in cat visual cortex: Inter-columnar interaction as determined by cross-correlation analysis. *European Journal of Neuroscience*, **2**, 588–606.

Feigenbaum, M. J. (1979). The universal metric properties of nonlinear transformations. *Journal of Statistical Physics*, **22**, 186–223.

Freeman, W. J. (1975). *Mass action in the nervous system*. New York: Academic Press.

Freeman, W. J. (1987). Simulation of chaotic EEG patterns with a dynamic model of the olfactory system. *Biological Cybernetics*, **56**, 139–150.

Freeman, W. J. (1990). On the problem of anomalous dispersion in chaoto-chaotic phase transitions of neural masses, and its significance for perceptual information in the brain. In H. Haken & M. Stadler (Eds.), *Synergetics of Cognition*, pp. 126–143. Berlin: Springer-Verlag.

Freeman, W. J. (1993). Deconstruction of neural data yields biologically implausible periodic oscillations. *Behavioral and Brain Sciences*, **16**, 458–459.

Gilden, D. L., Schmuckler, M. A., & Clayton, K. (1993). The perception of natural contour. *Psychological Review*, **100**, 460–478.

Goldstone, R. L., & Medin, D. L. (1994). Time course of comparison. *Journal of Experimental Psychology*: *Learning*, *Memory and Cognition*, **20**, 29–50.

Gray, C. M., & Singer, W. (1989). Stimulus specific neuronal oscillations in orientation columns of cat visual cortex. *Proceedings of the National Academy of Sciences USA*, **86**, 1698–1702.

Gray, C. M., Engel, A. K., König, P., & Singer, W. (1990). Stimulus-dependent neuronal oscillations in cat visual cortex: receptive field properties and feature dependence. *European Journal of Neuroscience*, **2**, 607–619.

Green, D. M., & Swets, J. A. (1966). *Signal Detection Theory and Psychophysics*. New York: Wiley.

Gregson, R. A. M. (1988). *Nonlinear psychophysical dynamics*. Hillsdale, NJ: Lawrence Erlbaum Associates.

Grossberg, S., & Mingolla, E. (1985). Neural dynamics of form perception: Boundary completion, illusory figures and neon color spreading. *Psychological Review*, **92**, 173–211.

Grossberg, S., & Somers, D. (1991). Synchronized oscillations during cooperative feature linking in a cortical model of visual perception. *Neural Networks*, **4**, 453–466.

Gu, Y., Tung, M., Yuan, J. M., Feng, D. H., & Narducci, L. M. (1984). Crises and hysteresis in coupled logistic maps. *Physical Review Letters*, **52**, 701–704.

Haken, H., & Stadler, M. (1990). *Synergetics of Cognition*. Berlin: Springer-Verlag.

Henderson, J. M. (1992). Object identification in context: The visual processing of natural scenes. *Canadian Journal of Psychology*, **46**, 319–341.

Hinton, G. E. (1981). Shape representation in parallel systems. In *Proceedings of the 7th International Joint conference on Artificial Intelligence*, *Vancouver*, *BC*, *Canada*, pp. 1088–1096.

Hock, H. S., Kelso, J. A. S., & Schöner, G. (1993). Bistability and hysteresis in the organization of apparent motion patterns. *Journal of Experimental Psychology*: *Human Perception and Performance*, **19**, 63–80.

Hoffman, D. D., & Richards, W. A. (1984). Parts of recognition. Special issue: Visual cognition. *Cognition*, **18**, 65–96.

Hoffman, W. C. (1989). The visual cortex is a contact bundle. *Applied Mathematics and Computation*, **32**, 137–167.

Hogeboom, M., & van Leeuwen, C. (1997). Visual search strategy and perceptual organization covary with individual preference and structural complexity. *Acta Psychologica*, **95**, 141–164.

Hogg, T., & Huberman, B. A. (1984). Generic behavior of coupled oscillators. *Physical Review A*, **29**, 275–281.

Hopfield, J. J. (1982). Neural networks and physical systems with emergent collective computational abilities. *Proceedings of the National Academy of Sciences*, **79**, 2554–2558.

Kaneko, K. (1983). Transition from torus to chaos accompanied by frequency lockings with symmetry breaking. *Progress of Theoretical Physics*, **69**, 1427–1442.

Kaneko, K. (1984). Period-doubling of kink–antikink patterns, quasi-periodicity in antiferro-like structures and spatial intermittency in coupled logistic lattice. *Progress of Theoretical Physics*, **72**, 480–486.

Kaneko, K. (1989). Chaotic but regular posi–nega switch among coded attractor by cluster-size variation. *Physical Review Letters*, **63**, 219–223.

Kaneko, K. (1990). Clustering, coding, switching, hierarchical ordering, and control in a network of chaotic elements. *Physica D*, **41**, 137–172.

Kanizsa, G., & Luccio, R. (1990). The phenomenology of autonomous order formation in perception. In H. Haken & M. Stadler (Eds.), *Synergetics of Cognition*, pp. 186–200. Berlin: Springer-Verlag.

Kawamoto, A. H., & Anderson, J. A. (1985). A neural network model of multistable perception. *Acta Psychologica*, **59**, 35–65.

Kelso, J. A. S. (1995). *Dynamic Patters. The Self-Organization of Brain and Behavior*. Cambridge, MA: MIT Press.

Köhler, (1940). *Dynamics in Psychology*. *Vital Applications of Gestalt Psychology*. New York: Liveright.

May, R. M. (1974). Biological populations with nonoverlapping generations: Stable points, stable cycles, and chaos. *Science*, **186**, 645–647.

Martindale, C. (1995). Creativity and connectionism. In S. M. Smith, Th. B. Ward, & R. Finke (Eds.), *The Creative Cognition Approach*, pp. 249–268. Cambridge, MA: MIT Press.

Norton, A. (1995). Dynamics: An introduction. In R. F. Port & T. Van Gelder (Eds.), *Mind as Motion. Exploration in the Dynamics of Cognition*, pp. 45–68. Boston, MA: MIT Press.

Palmer, S., & Rock, I. (1994). Rethinking perceptual organization: The role of uniform connectedness. *Psychonomic Bulletin & Review*, **1**, 29–55.

Pecora, L. M., & Carroll, T. L. (1990). Synchronization in chaotic systems. *Physical Review Letters*, **64**, 821–824.

Peterson, M. A., & Hochberg, J. (1983). Opposed-set measurement procedure: A quantitative analysis of the role of local cues and intention in form perception. *Journal of Experimental Psychology*: *Human Perception and Performance*, **9**, 183–193.

Pomerantz, J. R., & Garner, W. R. (1973). Stimulus configuration in selective attention tasks. *Perception & Psychophysics*, **14**, 565–569.

Pomerantz, J. R., & Pristach, E. A. (1989). Emergent features, attention and perceptual glue in visual form perception. *Journal of Experimental Psychology*: *Human Perception and Performance*, **15**, 635–649.

Schult, R. L., Creamer, D. B., Henyey, F. S., & Wright, J. A., (1987). Symmetric and non-symmetric coupled logistic maps. *Physical Review A*, **35**, 3115–3118.

Sekuler, A. B., & Palmer, S. E. (1992). Perception of partly occluded objects: A microgenetic analysis. *Journal of Experimental Psychology*: *General*, **121**, 95–111.

Shannon, C. E., & Weaver, W. (1949). *The Mathematical Theory of Communication*. Urbana, IL: University of Illinois Press.

Skarda, C. A., & Freeman, W. J. (1987). How brains make chaos to make sense of the world. *Behavioral and Brain Sciences*, **10**, 161–195.

Sompolinsky, H., & Golomb, D. (1991). Cooperative dynamics in visual processing. *Physical Review A*, **43**, 6990–7011.

Sompolinsky, H., Golomb, D., & Kleinfeld, D. (1990). Global processing of visual stimuli in a neural network of coupled oscillators. *Proceedings of the National Academy of Sciences USA*, **87**, 7200–7204.

Sprons, O., Gally, J. A., Reeke, G. N., Jr., & Edelman, G. M. (1989). Reentrant signaling among simulated neuronal groups leads to coherency in their oscillatory activity. *Proceedings of the National Academy of Sciences USA*, **86**, 7265–7269.

Sporns, O., Tononi, G., & Edelman, G. M. (1991). Modeling perceptual grouping and figure–ground segregation by means of active reentrant

connections. *Proceedings of the National Academy of Sciences USA*, **88**, 129–133.

Taylor, M. M., & Aldridge, K. D. (1974). Stochastic processes in reversing figure perception. *Perception & Psychophysics*, **16**, 9–27.

Tsuda, I. (1992). Dynamic link of memory-chaotic memory map to nonequilibrium neural networks. *Neural Networks*, **5**, 313–326.

Tsuda, I. (1993). Dynamic-binding theory is not plausible without chaotic oscillation. *Behavioral and Brain Sciences*, **16**, 475–476.

van Leeuwen, C. (1989). PDP and Gestalt, an Integration? *Psychological Research*, **50**, 199–201.

van Leeuwen, C. (in press). Visual perception on the edge of chaos. In S. Jordan (Ed.), *Systems Theory and Apriori aspects of Perception*. Amsterdam: Elsevier Science.

van Leeuwen, C., & Bakker, L. (1995). Stroop can occur without Garner interference: Strategic and mandatory influences in multidimensional stimuli. *Perception & Psychophysics*, **57**, 379–392.

van Leeuwen, C., Buffart, H., & van der Vegt, J. (1988). Sequence influence on the organization of meaningless serial stimuli: Economy after all. *Journal of Experimental Psychology: Human Perception and Performance*, **14**, 481–502.

van Oeffelen, M. P., & Vos, P. G. (1982). Configurational effects on the enumeration of dots: Counting by groups. *Memory & Cognition*, **10**, 396–404.

Von der Malsburg, C., & Schneider, W. (1986). A neural cocktail-party processor. *Biological Cybernetics*, **54**, 29–40.

Waller, I., & Kapral, R. (1984). Spatial and temporal structure in systems of coupled nonlinear oscillators. *Physical Review A*, **30**, 2049–2055.

Yamada, T., & Fujisaka, H. (1983). Stability theory of synchronized motion in coupled-oscillator systems. *Progress of Theoretical Physics*, **70**, 1240–1248.

Received: January 25, 1995